Eur. Phys. J. C 20, 283–300 (2001)
Digital Object Identifier (DOI) 10.1007/s100520100674

THE EUROPEAN PHYSICAL JOURNAL C

# Factorization scheme and parton distributions in the polarized virtual photon target

K. Sasaki[1,2,a], T. Uematsu[1,2,b]

[1] Department of Physics, Faculty of Engineering, Yokohama National University, Yokohama 240-8501, Japan
[2] Department of Fundamental Sciences, FIHS, Kyoto University, Kyoto 606-8501, Japan

Received: 24 January 2001 /
Published online: 18 May 2001 – 

**Abstract.** We investigate spin-dependent parton distributions in the polarized virtual photon target in perturbative QCD up to the next-to-leading order (NLO). In the case $\Lambda^2 \ll P^2 \ll Q^2$, where $-Q^2$ $(-P^2)$ is the mass squared of the probe (target) photon, the parton distributions can be predicted completely up to NLO, but they are factorization-scheme dependent. We analyze the parton distributions in six different factorization schemes and discuss their scheme dependence. We study, in particular, the QCD and QED axial anomaly effects on the first moments of the parton distributions to see the interplay between the axial anomalies and factorization schemes. We also show that the factorization-scheme dependence is characterized by the large-$x$ behaviors of the quark distributions in the virtual photon. The gluon distribution is predicted to be the same up to NLO among the six factorization schemes examined. In particular, the first moment of the gluon distribution is found to be factorization-scheme independent up to NLO.

## 1 Introduction

In the two-photon process of $e^+e^-$ collision experiments, we can measure the structure functions of the virtual photon (Fig. 1). The advantage in studying the virtual photon target is that in case

$$\Lambda^2 \ll P^2 \ll Q^2, \tag{1.1}$$

where $-Q^2$ $(-P^2)$ is the mass squared of the probe (target) photon and $\Lambda$ is the QCD scale parameter, we can calculate the whole structure function up to the next-to-leading order (NLO) in QCD by the perturbative method, in contrast to the case of a real photon target where in NLO there exist non-perturbative pieces [1,2]. The spin-independent structure functions $F_2^\gamma(x, Q^2, P^2)$ and $F_L^\gamma(x, Q^2, P^2)$ as well as the parton contents were studied in the leading order (LO) [3] and in NLO [4–9]. The target mass effect of an unpolarized and a polarized virtual photon structure in LO was discussed in [10].

The information on the spin structure of the photon would be provided by the resolved photon process in the polarized version of the DESY electron and proton collider HERA [11,12]. More directly, the polarized photon structure function can be measured by polarized $e^+e^-$ collisions in the future linear colliders. For the real photon $(P^2 = 0)$ target, there exists only one spin-dependent structure function, $g_1^\gamma(x, Q^2)$, which is equivalent to the structure function $W_4^\gamma(x, Q^2)$ $(g_1^\gamma \equiv 2W_4^\gamma)$ discussed some time ago in [13,14]. The LO QCD corrections to $g_1^\gamma$ for the real photon target was first calculated by one of the authors [15] and later in [16,17], while the NLO QCD analysis was performed by Stratmann and Vogelsang [18]. The first moment of the photon structure function $g_1^\gamma$ has recently attracted attention in the literature [17,19–22] in connection with its relevance for the axial anomaly. More recently the present authors investigated [23] the spin-dependent structure function $g_1^\gamma(x, Q^2, P^2)$ of the virtual

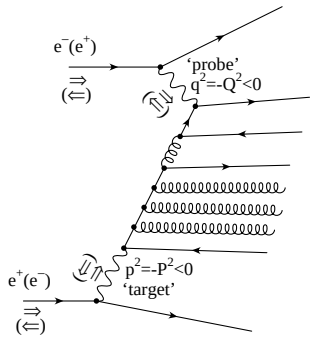


**Fig. 1.** Deep inelastic scattering on a polarized virtual photon in polarized $e^+e^-$ collision, $e^+e^- \to e^+e^-+$ hadrons (quarks and gluons). The arrows indicate the polarizations of the $e^+$, $e^-$ and the virtual photons. The mass squared of the "probe" ("target") photon is $-Q^2$ $(-P^2)$ $(\Lambda^2 \ll P^2 \ll Q^2)$

[a] e-mail: sasaki@phys.ynu.ac.jp
[b] e-mail: uematsu@phys.h.kyoto-u.ac.jp

photon up to NLO in QCD, where $P^2$ is in the above kinematical region, (1.1). The analysis was made in the framework of the operator product expansion (OPE) supplemented by the renormalization group method and also in the framework of the QCD improved parton model [24] using the DGLAP parton evolution equations.

In the past few years, the accuracy of the experimental data on the spin-dependent structure function $g_1$ of the nucleon has significantly been improved [25]. Using these experimental data together with the already existing world data, several groups [26–29] have carried out NLO QCD analyses of the polarized parton distributions in the nucleon. These parton distributions may be used for predicting the behaviors of other processes such as polarized Drell–Yan reactions and polarized semi-inclusive deep inelastic scatterings, etc. However, parton distributions obtained from the NLO analyses are dependent on the factorization scheme employed. It is possible that parton distributions obtained in one scheme may be more appropriate to use than those in other schemes. In the case of a nucleon target, however, it may be difficult to examine the features of each factorization scheme, since for the moment it is inevitable to resort to some assumptions in order to extract parton distributions from the experimental data.

On the other hand, it is remarkable that, in the case of a virtual photon target with the virtual mass $-P^2$ being in the kinematical region of (1.1), not only the photon structure functions but also the parton distributions in the target can be predicted entirely up to NLO in QCD. Thus, comparing the parton distributions predicted by one scheme with those by other schemes, we can easily examine the features of each factorization scheme. In consequence, the virtual photon target may serve as an optimal place to study the behaviors of the parton distributions and their factorization-scheme dependences.

In this paper we examine in detail the polarized parton (i.e., quark and gluon) distributions in the virtual photon target. The polarized parton distributions are particularly interesting due to the fact that they have relevance for the axial anomaly [30]. The interplay between the QCD axial anomaly and the factorization schemes has already been discussed for the spin-dependent structure function $g_1$ of the nucleon [31–37]. It was explained there that the QCD axial anomaly effect is retained in the flavor singlet quark distribution in the nucleon in the standard $\overline{\rm MS}$ scheme, but it is shifted to the gluon coefficient function in a scheme such as the one called the chirally invariant (CI) factorization scheme. Now it should be pointed out that the polarized photon target is unique in the sense that not only QCD but also the OED axial anomaly occurs. The QED axial anomaly, which is an $U(1)$ anomaly, emerges when a quark has an electromagnetic charge. Thus the flavor-non-singlet quark distribution is also relevant, besides the flavor singlet one. Depending upon the factorization schemes, the QED axial anomaly effect resides in both the flavor singlet and non-singlet polarized quark distributions in the virtual photon, or it is shifted to the photon coefficient function, in which case we arrive at an interesting result: the first moments of the polarized quark distributions in the virtual photon, both flavor singlet and non-singlet, vanish in NLO. Also we find that the large-$x$ behaviors of the polarized quark distributions dramatically vary from one factorization scheme to another. Indeed, for $x \to 1$, the quark distributions positively diverge or negatively diverge or remain finite, depending on the factorization schemes.

We perform our analyses in six different factorization schemes: (i) $\overline{\rm MS}$, (ii) CI (chirally invariant) (also called JET) [37,38], (iii) AB (Adler–Bardeen) [36], (iv) OS (off-shell) [36], (v) AR (Altarelli–Ross) [36], and finally (vi) DIS$_\gamma$ schemes [39], and we will see how the parton distributions change in each scheme. In particular, we study the axial anomaly effects on the first moments and the large-$x$ behaviors of the parton distributions. The gluon distribution in the virtual photon is found to be the same up to NLO, at least among the factorization schemes considered in this paper. Furthermore, the first moment of the gluon distribution turns out to be factorization-scheme independent up to NLO. Part of this result has been briefly reported elsewhere [40].

In the next section we discuss the polarized parton distributions in the virtual photon. The explicit expressions for the flavor singlet (non-singlet) quark and gluon distributions predicted in QCD up to NLO are given in Appendix A. In Sect. 3, we derive the transformation rules for the relevant two-loop anomalous dimensions and one-loop photon matrix elements from the $\overline{\rm MS}$ scheme to other factorization schemes and then explain the particular factorization schemes we consider in this paper. In Sect. 4, we examine the first moments of the parton distributions with emphasis on the interplay between the QCD and QED axial anomalies and the factorization schemes. The behaviors of the parton distributions near $x = 1$ and their factorization-scheme dependence are discussed in Sect. 5. The numerical analyses of the parton distributions predicted by the different factorization schemes will be given in Sect. 6. The final section is devoted to the conclusion and the discussion.

## 2 Polarized parton distributions in the photon

Let $q^i_\pm(x,Q^2,P^2)$, $G^\gamma_\pm(x,Q^2,P^2)$, $\Gamma^\gamma_\pm(x,Q^2,P^2)$ be the quark (with $i$-flavor), gluon, and photon distribution functions with $\pm$ helicities of the longitudinally polarized virtual photon with mass $-P^2$. Then the spin-dependent parton distributions are defined as $\Delta q^i \equiv q^i_+ + \bar{q}^i_+ - q^i_- - \bar{q}^i_-$, $\Delta G^\gamma \equiv G^\gamma_+ - G^\gamma_-$, and $\Delta\Gamma^\gamma \equiv \Gamma^\gamma_+ - \Gamma^\gamma_-$. In the leading order of the electromagnetic coupling constant, $\alpha = e^2/4\pi$, $\Delta\Gamma^\gamma$ does not evolve with $Q^2$ and is set to be $\Delta\Gamma^\gamma(x,Q^2,P^2) = \delta(1-x)$. For later convenience we use, instead of $\Delta q^i$, the flavor singlet and non-singlet combinations of the spin-dependent quark distributions as follows:

$$\Delta q^\gamma_{\rm S} \equiv \sum_i \Delta q^i,$$
$$\Delta q^\gamma_{\rm NS} \equiv \sum_i e_i^2 \left( \Delta q^i - \frac{\Delta q^\gamma_{\rm S}}{N_f} \right). \tag{2.1}$$

In terms of these parton distributions, the polarized virtual photon structure function $g_1^\gamma(x,Q^2,P^2)$ is expressed in the QCD improved parton model as [23]

$$\begin{aligned} & g_1^\gamma(x,Q^2,P^2) \\ &= \int_x^1 \frac{\mathrm{d}y}{y}\left\{\Delta q_{\mathrm{S}}^\gamma(y,Q^2,P^2)\Delta C_{\mathrm{S}}^\gamma\left(\frac{x}{y},Q^2\right)\right. \\ &\quad +\Delta G^\gamma(y,Q^2,P^2)\Delta C_G^\gamma\left(\frac{x}{y},Q^2\right)+\Delta q_{\mathrm{NS}}^\gamma(y,Q^2,P^2) \\ &\quad \left.\times\,\Delta C_{\mathrm{NS}}^\gamma\left(\frac{x}{y},Q^2\right)\right\}+\Delta C_\gamma^\gamma(x,Q^2), \end{aligned} \tag{2.2}$$

where $\Delta C_{\mathrm{S}}^\gamma(\Delta C_{\mathrm{NS}}^\gamma)$, $\Delta C_G^\gamma$, and $\Delta C_\gamma^\gamma$ are the coefficient functions corresponding to the singlet (non-singlet) quark, gluon, and photon, respectively, and these are independent of $P^2$. The Mellin moments of $g_1^\gamma$ are written as

$$g_1^\gamma(n,Q^2,P^2)=\Delta\widetilde{\boldsymbol{C}}^\gamma(n,Q^2)\cdot\Delta\widetilde{\boldsymbol{q}}^\gamma(n,Q^2,P^2), \tag{2.3}$$

where

$$\begin{aligned} \Delta\widetilde{\boldsymbol{C}}^\gamma(n,Q^2)&=(\Delta C_{\mathrm{S}}^\gamma,\Delta C_G^\gamma,\Delta C_{\mathrm{NS}}^\gamma,\Delta C_\gamma^\gamma),\\ \Delta\widetilde{\boldsymbol{q}}^\gamma(n,Q^2,P^2)&=(\Delta q_{\mathrm{S}}^\gamma,\Delta G^\gamma,\Delta q_{\mathrm{NS}}^\gamma,\Delta\Gamma^\gamma), \end{aligned}$$

and the matrix notation is implicit.

The explicit expressions of $\Delta q_{\mathrm{S}}^\gamma$, $\Delta G^\gamma$, and $\Delta q_{\mathrm{NS}}^\gamma$ up to NLO can be derived from (4.46) of [23], which are given in Appendix A. They are written[1] in terms of one- (two-) loop hadronic anomalous dimensions $\Delta\gamma_{ij}^{0,n}$ ($\Delta\gamma_{ij}^{(1),n}$) ($i,j=\psi,G$) and $\Delta\gamma_{\mathrm{NS}}^{0,n}$ ($\gamma_{\mathrm{NS}}^{(1),n}$), one- (two-) loop anomalous dimensions $\Delta K_i^{0,n}$ ($\Delta K_i^{(1),n}$) ($i=\psi,G,\mathrm{NS}$) which represent the mixing between photon and three hadronic operators $R_i^n$ ($i=\psi,G,\mathrm{NS}$), and finally $\Delta A_i^n$, the one-loop photon matrix elements of the hadronic operators renormalized at $\mu^2=P^2(=-p^2)$,

$$\langle\gamma(p)\mid R_i^n(\mu)\mid\gamma(p)\rangle|_{\mu^2=P^2}=\frac{\alpha}{4\pi}\Delta A_i^n\quad(i=\psi,G,\mathrm{NS}). \tag{2.4}$$

The photon matrix elements $\Delta A_i^n$ are scheme-dependent. In one-loop order, they are given, in the $\overline{\mathrm{MS}}$ scheme, by [34]

$$\begin{aligned} \Delta A_{\psi,\overline{\mathrm{MS}}}^n &= \frac{\langle e^2\rangle}{\langle e^4\rangle-\langle e^2\rangle^2}\Delta A_{\mathrm{NS},\overline{\mathrm{MS}}}^n \\ &= 12\langle e^2\rangle N_f\left\{\frac{n-1}{n(n+1)}S_1(n)+\frac{4}{(n+1)^2}\right. \\ &\quad \left.-\frac{1}{n^2}-\frac{1}{n}\right\}, \\ \Delta A_{G,\overline{\mathrm{MS}}}^n &= 0, \end{aligned} \tag{2.5}$$

where $S_1(n)=\sum_{j=1}^n(1/j)$.

[1] We use the same notations as in [23], except that the symbol $\Delta$ has been appended to all the spin-dependent anomalous dimensions, coefficient functions and photon matrix elements

## 3 Factorization schemes

### 3.1 Rules for the transformation from the $\overline{\mathrm{MS}}$ scheme to the $a$-scheme

Although $g_1^\gamma$ is a physical quantity and thus is unique, there remains a freedom in the factorization of $g_1^\gamma$ into $\Delta\widetilde{\boldsymbol{C}}^\gamma$ and $\Delta\widetilde{\boldsymbol{q}}^\gamma$. Given the formula (2.3), we can always redefine $\Delta\widetilde{\boldsymbol{C}}^\gamma$ and $\Delta\widetilde{\boldsymbol{q}}^\gamma$ as follows [41]:

$$\begin{aligned} \Delta\widetilde{\boldsymbol{C}}^\gamma(n,Q^2)&\to\Delta\widetilde{\boldsymbol{C}}^\gamma(n,Q^2)|_a \\ &\equiv\Delta\widetilde{\boldsymbol{C}}^\gamma(n,Q^2)Z_a^{-1}(n,Q^2), \end{aligned} \tag{3.1}$$

$$\begin{aligned} \Delta\widetilde{\boldsymbol{q}}^\gamma(n,Q^2,P^2)&\to\Delta\widetilde{\boldsymbol{q}}(n,Q^2,P^2)|_a \\ &\equiv Z_a(n,Q^2)\Delta\widetilde{\boldsymbol{q}}^\gamma(n,Q^2,P^2), \end{aligned} \tag{3.2}$$

where $\Delta\widetilde{\boldsymbol{C}}^\gamma|_a$ and $\Delta\widetilde{\boldsymbol{q}}|_a$ correspond to the quantities in a new factorization scheme $a$. Note that the coefficient functions and anomalous dimensions are closely connected under factorization. We will study the factorization-scheme dependence of the parton distribution up to NLO, by which we mean that a scheme transformation for the coefficient functions is considered up to the one-loop order, since a NLO prediction for $g_1^\gamma$ is given by the one-loop coefficient functions and anomalous dimensions up to the two-loop order.

The most general form of a transformation for the coefficient functions in one-loop order, from the $\overline{\mathrm{MS}}$ scheme to a new factorization scheme $a$, is given by

$$\begin{aligned} \Delta C_{\mathrm{S},a}^{\gamma,n}&=\Delta C_{\mathrm{S},\overline{\mathrm{MS}}}^{\gamma,n}-\langle e^2\rangle\frac{\alpha_{\mathrm{s}}}{2\pi}\Delta w_{\mathrm{S}}(n,a),\\ \Delta C_{G,a}^{\gamma,n}&=\Delta C_{G,\overline{\mathrm{MS}}}^{\gamma,n}-\langle e^2\rangle\frac{\alpha_{\mathrm{s}}}{2\pi}\Delta z(n,a),\\ \Delta C_{\mathrm{NS},a}^{\gamma,n}&=\Delta C_{\mathrm{NS},\overline{\mathrm{MS}}}^{\gamma,n}-\frac{\alpha_{\mathrm{s}}}{2\pi}\Delta w_{\mathrm{NS}}(n,a),\\ \Delta C_{\gamma,a}^{\gamma,n}&=\Delta C_{\gamma,\overline{\mathrm{MS}}}^{\gamma,n}-\frac{\alpha}{\pi}3\langle e^4\rangle\Delta\hat{z}(n,a), \end{aligned} \tag{3.3}$$

where $\langle e^4\rangle=\sum_i e_i^4/N_f$. The flavor singlet (non-singlet) quark coefficient functions are expanded up to the one-loop order as

$$\begin{aligned} \Delta C_{\mathrm{S}}^{\gamma,n}&=\langle e^2\rangle\left(1+\frac{\alpha_{\mathrm{s}}}{4\pi}\Delta B_{\mathrm{S}}^n+\mathcal{O}(\alpha_{\mathrm{s}}^2)\right),\\ \Delta C_{\mathrm{NS}}^{\gamma,n}&=1+\frac{\alpha_{\mathrm{s}}}{4\pi}\Delta B_{\mathrm{NS}}^n+\mathcal{O}(\alpha_{\mathrm{s}}^2), \end{aligned} \tag{3.4}$$

with $\Delta B_{\mathrm{S}}^n=\Delta B_{\mathrm{NS}}^n$. The $\Delta z(n,a)$ ($\Delta\hat{z}(n,a)$) term tells how much of the QCD (QED) axial anomaly effect is transferred to the coefficient function in the new factorization scheme. The gluon and photon coefficient functions $\Delta C_G^{\gamma,n}$ and $\Delta C_\gamma^{\gamma,n}$ start from the one-loop order (i.e., from the NLO):

$$\begin{aligned} \Delta C_G^{\gamma,n}&=\langle e^2\rangle\left(\frac{\alpha_{\mathrm{s}}}{4\pi}\Delta B_G^n+\mathcal{O}(\alpha_{\mathrm{s}}^2)\right),\\ \Delta C_\gamma^{\gamma,n}&=\frac{\alpha}{4\pi}3N_f\langle e^4\rangle(\Delta B_\gamma^n+\mathcal{O}(\alpha_{\mathrm{s}})). \end{aligned} \tag{3.5}$$

In the $\overline{\mathrm{MS}}$ scheme, $\Delta C_{\gamma,\overline{\mathrm{MS}}}^{\gamma,n}$ has been obtained from $\Delta C_{G,\overline{\mathrm{MS}}}^{\gamma,n}$, but with changes: $\alpha_{\mathrm{s}}/2\pi\to(2\alpha/\alpha_{\mathrm{s}})\times(\alpha_{\mathrm{s}}/2\pi)$, $\langle e^2\rangle\to3\langle e^4\rangle$, and 3 is the number of colors. Thus we have

$$Z_a^{-1}(n,Q^2) = I - \begin{pmatrix} \frac{\alpha_s}{2\pi}\Delta w_S(n,a) & \frac{\alpha_s}{2\pi}\Delta z(n,a) & 0 & \frac{\alpha}{\pi}3\langle e^2\rangle\Delta\hat{z}(n,a) \\ 0 & 0 & 0 & 0 \\ 0 & 0 & \frac{\alpha_s}{2\pi}\Delta w_{NS}(n,a) & \frac{\alpha}{\pi}3(\langle e^4\rangle - \langle e^2\rangle^2)\Delta\hat{z}(n,a) \\ 0 & 0 & 0 & 0 \end{pmatrix}, \tag{3.8}$$

$$\Delta\widetilde{P}(n,Q^2) = \begin{pmatrix} \Delta P_{\psi\psi}(n,Q^2) & \Delta P_{\psi G}(n,Q^2) & 0 & \Delta k_S(n,Q^2) \\ \Delta P_{G\psi}(n,Q^2) & \Delta P_{GG}(n,Q^2) & 0 & \Delta k_G(n,Q^2) \\ 0 & 0 & \Delta P_{NS}(n,Q^2) & \Delta k_{NS}(n,Q^2) \\ 0 & 0 & 0 & 0 \end{pmatrix}. \tag{3.10}$$

$$\Delta B^n_{\gamma,\overline{\rm MS}} = \frac{2}{N_f}\Delta B^n_{G,\overline{\rm MS}}. \tag{3.6}$$

Since, in the leading order, the coefficient functions are given by

$$\Delta\boldsymbol{C}^\gamma_{\overline{\rm MS}}|_{\rm LO} = \Delta\boldsymbol{C}^\gamma_a|_{\rm LO} = (\langle e^2\rangle, 0, 1, 0), \tag{3.7}$$

the relations (3.3) between the coefficient functions in the $a$-scheme and the $\overline{\rm MS}$ scheme lead to $Z_a^{-1}(n,Q^2)$, which is expressed as (see (3.8) on top of page the page) where $I$ is a $4\times 4$ unit matrix.

Now we derive the corresponding rules for the transformation from the $\overline{\rm MS}$ scheme to the $a$-scheme for the relevant two-loop anomalous dimensions. The parton distribution functions $\Delta\widetilde{\boldsymbol{q}}^\gamma(n,Q^2,P^2)$ satisfy the following evolution equation [39,41–44]:

$$\frac{{\rm d}\Delta\widetilde{\boldsymbol{q}}^\gamma(n,Q^2,P^2)}{{\rm dln}Q^2} = \Delta\widetilde{P}(n,Q^2)\Delta\widetilde{\boldsymbol{q}}^\gamma(n,Q^2,P^2), \tag{3.9}$$

where (see (3.10) on top of the page) From (3.2) we obtain

$$\begin{aligned}\frac{{\rm d}\Delta\widetilde{\boldsymbol{q}}^\gamma(n,Q^2,P^2)|_a}{{\rm dln}Q^2} &= \frac{{\rm d}Z_a(n,Q^2)}{{\rm dln}Q^2}\Delta\widetilde{\boldsymbol{q}}^\gamma(n,Q^2,P^2)|_{\overline{\rm MS}} \\ &+ Z_a(n,Q^2)\frac{{\rm d}\Delta\widetilde{\boldsymbol{q}}^\gamma(n,Q^2,P^2)|_{\overline{\rm MS}}}{{\rm dln}Q^2} \\ &= \Delta\widetilde{P}(n,Q^2)|_a\Delta\widetilde{\boldsymbol{q}}^\gamma(n,Q^2,P^2)|_a,\end{aligned} \tag{3.11}$$

with

$$\begin{aligned}\Delta\widetilde{P}(n,Q^2)|_a = \Bigg[&\frac{{\rm d}Z_a(n,Q^2)}{{\rm dln}Q^2} \\ &+ Z_a(n,Q^2)\Delta\widetilde{P}(n,Q^2)|_{\overline{\rm MS}}\Bigg] Z_a^{-1}(n,Q^2).\end{aligned} \tag{3.12}$$

The splitting functions $\Delta P_i(n,Q^2)$ ($i=\psi\psi,\psi G,G\psi,GG$, and NS) and $\Delta k_j(n,Q^2)$ ($j={\rm S},G,{\rm NS}$) are expanded as

$$\begin{aligned}\Delta P_i(n,Q^2) &= \frac{\alpha_s(Q^2)}{2\pi}\Delta P_i^{(0)}(n) \\ &+ \left[\frac{\alpha_s(Q^2)}{2\pi}\right]^2\Delta P_i^{(1)}(n) + \cdots,\end{aligned} \tag{3.13}$$

$$\Delta k_j(n,Q^2) = \frac{\alpha}{2\pi}\Delta k_j^{(0)}(n) + \frac{\alpha\alpha_s(Q^2)}{(2\pi)^2}\Delta k_j^{(1)}(n) + \cdots \tag{3.14}$$

Since the QCD effective coupling constant $\alpha_s(Q^2)$ satisfies

$$\frac{{\rm d}\alpha_s(Q^2)}{{\rm dln}Q^2} = -\beta_0\frac{\alpha_s(Q^2)^2}{4\pi} + \cdots, \tag{3.15}$$

where $\beta_0 = 11-(2/3)N_f$ is the one-loop coefficient of the QCD beta function, and the $n$th anomalous dimensions are defined as

$$\Delta P_i^{(0)}(n) = -\frac{1}{4}\Delta\gamma_i^{0,n}, \quad \Delta P_i^{(1)}(n) = -\frac{1}{8}\Delta\gamma_i^{(1),n}, \tag{3.16}$$

$$\Delta k_j^{(0)}(n) = \frac{1}{4}\Delta K_j^{0,n}, \quad \Delta k_j^{(1)}(n) = \frac{1}{8}\Delta K_j^{(1),n}, \tag{3.17}$$

we find for one loop

$$\Delta\gamma_{i,a}^{0,n} = \Delta\gamma_{i,\overline{\rm MS}}^{0,n}, \quad \Delta K_{j,a}^{0,n} = \Delta K_{j,\overline{\rm MS}}^{0,n}, \tag{3.18}$$

and for two loops

$$\begin{aligned}
\Delta\gamma_{\psi\psi,a}^{(1),n} &= \Delta\gamma_{\psi\psi,\overline{\rm MS}}^{(1),n} + 2\Delta z(n,a)\Delta\gamma_{G\psi}^{0,n} + 4\beta_0\Delta w_S(n,a), \\
\Delta\gamma_{\psi G,a}^{(1),n} &= \Delta\gamma_{\psi G,\overline{\rm MS}}^{(1),n} + 2\Delta z(n,a)[\Delta\gamma_{GG}^{0,n} - \Delta\gamma_{\psi\psi}^{0,n} + 2\beta_0] \\
&\quad + 2\Delta w_S(n,a)\Delta\gamma_{\psi G}^{0,n}, \\
\Delta\gamma_{G\psi,a}^{(1),n} &= \Delta\gamma_{G\psi,\overline{\rm MS}}^{(1),n} - 2\Delta w_S(n,a)\Delta\gamma_{G\psi}^{0,n}, \\
\Delta\gamma_{GG,a}^{(1),n} &= \Delta\gamma_{GG,\overline{\rm MS}}^{(1),n} - 2\Delta z(n,a)\Delta\gamma_{G\psi}^{0,n}, \\
\Delta\gamma_{{\rm NS},a}^{(1),n} &= \Delta\gamma_{{\rm NS},\overline{\rm MS}}^{(1),n} + 4\beta_0\Delta w_{NS}(n,a), \\
\Delta K_{{\rm S},a}^{(1),n} &= \Delta K_{{\rm S},\overline{\rm MS}}^{(1),n} + 2\Delta w_S(n,a)\Delta K_{\rm S}^{0,n} \\
&\quad + 4\Delta\hat{z}(n,a)3\langle e^2\rangle\Delta\gamma_{\psi\psi}^{0,n}, \\
\Delta K_{G,a}^{(1),n} &= \Delta K_{G,\overline{\rm MS}}^{(1),n} + 4\Delta\hat{z}(n,a)3\langle e^2\rangle\Delta\gamma_{G\psi}^{0,n}, \\
\Delta K_{{\rm NS},a}^{(1),n} &= \Delta K_{{\rm NS},\overline{\rm MS}}^{(1),n} + 2\Delta w_{NS}(n,a)\Delta K_{\rm NS}^{0,n} \\
&\quad + 4\Delta\hat{z}(n,a)3(\langle e^4\rangle - \langle e^2\rangle^2)\Delta\gamma_{\rm NS}^{0,n}.
\end{aligned} \tag{3.19}$$

The one-loop photon matrix elements of the hadronic operators, $\Delta A_\psi^n$ and $\Delta A_{\rm NS}^n$ in (2.4), are related to each other by

$$\Delta A_{\rm NS}^n = \Delta A_\psi^n\frac{\langle e^4\rangle - \langle e^2\rangle^2}{\langle e^2\rangle}, \tag{3.20}$$

and the sum

$$\left(\Delta C_\gamma^{\gamma,n}/\frac{\alpha}{4\pi} + \langle e^2\rangle\Delta A_\psi^n + \Delta A_{\rm NS}^n\right) \tag{3.21}$$

is factorization-scheme independent in one-loop order [23]. Thus we obtain from (3.3)

$$\begin{aligned}\Delta A^n_{\psi,a} &= \Delta A^n_{\psi,\overline{\rm MS}} + 12\langle e^2\rangle \Delta\hat{z}(n,a),\\ \Delta A^n_{G,a} &= \Delta A^n_{G,\overline{\rm MS}} = 0,\\ \Delta A^n_{{\rm NS},a} &= \Delta A^n_{{\rm NS},\overline{\rm MS}} + 12(\langle e^4\rangle - \langle e^2\rangle^2)\Delta\hat{z}(n,a).\end{aligned} \tag{3.22}$$

Note that $\Delta A^n_G = 0$ in one-loop order.

It is possible to choose $\Delta z(n,a)$ and $\Delta\hat{z}(n,a)$ arbitrarily. In the following, we take $\Delta\hat{z}(n,a) = \Delta z(n,a)$ in the CI-like schemes and $\Delta\hat{z}(n,{\rm DIS}_\gamma) \neq \Delta z(n,{\rm DIS}_\gamma) = 0$ in the ${\rm DIS}_\gamma$ scheme. In one-loop order we have $\Delta w_{\rm S}(n,a) = \Delta w_{\rm NS}(n,a)$. Thus from now on we set $\Delta w_{\rm S}(n,a) = \Delta w_{\rm NS}(n,a) \equiv \Delta w(n,a)$. Let us now discuss the features of several factorization schemes.

### 3.2 The $\overline{\rm MS}$ scheme

This is the only scheme in which both relevant one-loop coefficient functions and two-loop anomalous dimensions were actually calculated [34, 45–47]. In fact, there still remain ambiguities in the $\overline{\rm MS}$ scheme, depending on how to handle $\gamma_5$ in $n$ dimensions. The $\overline{\rm MS}$ scheme we have here is the one due to Mertig and van Neerven [46] and Vogelsang [47], in which the first moment of the non-singlet quark operator vanishes, corresponding to the conservation of the non-singlet axial current. Indeed, we have $\Delta\gamma^{(1),n=1}_{{\rm NS},\overline{\rm MS}} = 0$. Explicit expressions of the relevant one-loop coefficient functions and two-loop anomalous dimensions can be found, for example, in the appendix of [23]. It is noted that in the $\overline{\rm MS}$ scheme both the QCD and QED axial anomalies reside in the quark distributions and not in the gluon and photon coefficient functions. In fact, we observe

$$\Delta\gamma^{(1),n=1}_{\psi\psi,\overline{\rm MS}} = 24 C_F T_f \neq 0, \tag{3.23}$$

$$\Delta B^{n=1}_{G,\overline{\rm MS}} = \Delta B^{n=1}_{\gamma,\overline{\rm MS}} = 0. \tag{3.24}$$

where $C_F = 4/3$ and $T_f = N_f/2$. Also we find from (2.5) that the first moments of the one-loop photon matrix elements of the quark operators get non-zero values, i.e.,

$$\Delta A^{n=1}_{\psi,\overline{\rm MS}} = \frac{\langle e^2\rangle}{\langle e^4\rangle - \langle e^2\rangle^2}\Delta A^{n=1}_{{\rm NS},\overline{\rm MS}} = -12\langle e^2\rangle N_f, \tag{3.25}$$

which is due to the QED axial anomaly.

### 3.3 The CI-like schemes

The EMC measurement [48] of the first moment of the proton spin structure function $g^p_1(x,Q^2)$ presented us with the issue called the "proton spin crisis". Since then many ideas have been proposed as solutions. One simple and plausible explanation was that there exists an anomalous gluon contribution to the first moment [31–33] originating from the QCD axial anomaly. This explanation was later [34] supported with the notion of the factorization-scheme dependence. There is a set of factorization schemes in which we obtain

$$\Delta B^{n=1}_G = -2N_f, \quad \Delta\gamma^{(1),n=1}_{\psi\psi} = 0. \tag{3.26}$$

Let us call these CI-like schemes. In this paper we consider four CI-like schemes, in which we take $\Delta z(n,a) = \Delta\hat{z}(n,a)$, since both QCD and QED anomalies originate from similar triangle diagrams. With this choice, the relation between the one-loop gluon and photon coefficient functions, which holds in the $\overline{\rm MS}$ scheme, also holds in the CI-like schemes,

$$\Delta B^n_{\gamma,{\rm CI-like}} = \frac{2}{N_f}\Delta B^n_{G,{\rm CI-like}}. \tag{3.27}$$

Thus, in addition to the relations in (3.26), we obtain in the CI-like schemes

$$\Delta B^{n=1}_{\gamma,{\rm CI-like}} = -4, \quad \Delta A^{n=1}_{\psi,{\rm CI-like}} = \Delta A^{n=1}_{{\rm NS},{\rm CI-like}} = 0. \tag{3.28}$$

(i) The chirally invariant (CI) scheme. In this scheme the factorization of the photon–gluon (photon–photon) cross section into the hard and soft parts is made so that chiral symmetry is respected [37, 38] and the QCD and QED anomaly effects are absorbed into the gluon and photon coefficient functions. Thus the spin-dependent quark distributions in the CI scheme are anomaly-free. The transformation from the $\overline{\rm MS}$ scheme to the CI scheme is achieved by

$$\begin{aligned}&\Delta w(n,a={\rm CI}) = 0,\\ &\Delta z(n,a={\rm CI}) = \Delta\hat{z}(n,a={\rm CI}) = 2N_f\frac{1}{n(n+1)}.\end{aligned} \tag{3.29}$$

It has been argued by Cheng [37] and Müller and Teryaev [38] that the $x$-dependence of the axial anomaly effect is uniquely fixed and that its $x$-behavior leads to the transformation rule (3.29) and thus to the CI scheme.

(ii) The Adler–Bardeen (AB) scheme. Ball, Forte and Ridolfi [36] proposed several CI-like schemes for the analysis of the nucleon spin structure function $g_1(x,Q^2)$. One of them is the Adler–Bardeen (AB) scheme which was introduced by requiring that the change from the $\overline{\rm MS}$ scheme to this scheme be independent of $x$, so that the large- and small-$x$ behavior of the gluon coefficient function is unchanged. In our case, we have in moment space

$$\begin{aligned}&\Delta w(n,a={\rm AB}) = 0,\\ &\Delta z(n,a={\rm AB}) = \Delta\hat{z}(n,a={\rm AB}) = N_f\frac{1}{n}.\end{aligned} \tag{3.30}$$

(iii) The off-shell (OS) scheme. In this scheme [36] we renormalize operators while keeping the incoming particle off shell, $p^2 \neq 0$, so that at the renormalization (factorization) point, $\mu^2 = -p^2$, the finite terms vanish. This is exactly the same as "the momentum subtraction scheme" which was used some time ago to calculate, for instance, the polarized quark and gluon coefficient functions [49,

30]. The CI-relations in (3.26) and (3.28) also hold in the OS scheme[2], since the axial anomaly appears as a finite term in the calculation of the triangle graph for $j_5^\mu$ between the external gluons (photons) and the finite term is thrown away in this scheme. The transformation from the $\overline{\rm MS}$ scheme to the OS scheme is made by choosing

$$\begin{aligned}\Delta w(n,a=\mathrm{OS}) &= C_F\left\{[S_1(n)]^2+3S_2(n)\right.\\ &\quad -S_1(n)\left(\frac{1}{n}-\frac{1}{(n+1)}\right)\\ &\quad \left.-\frac{7}{2}+\frac{2}{n}-\frac{3}{n+1}-\frac{1}{n^2}+\frac{2}{(n+1)^2}\right\},\\ \Delta z(n,a=\mathrm{OS}) &= \Delta\hat{z}(n,a=\mathrm{OS})\\ &= N_f\left\{-\frac{n-1}{n(n+1)}S_1(n)+\frac{1}{n}\right.\\ &\quad \left.+\frac{1}{n^2}-\frac{4}{(n+1)^2}\right\}. \end{aligned}\tag{3.31}$$

It is noted that in the OS scheme we have $\Delta A^n_{\psi,\mathrm{OS}} = \Delta A^n_{\mathrm{NS,OS}} = 0$ not only for $n=1$ but for all $n$.

(iv) The Altarelli–Ross (AR) scheme. Using a massive quark as a regulator for collinear divergence, Altarelli and Ross [31,50] derived the same one-loop gluon coefficient function $\Delta C_G^\gamma$ as in the case of the CI scheme. In order to obtain the one-loop quark coefficient function in this scheme, however, we need to do an extra subtraction so that the conservation of the non-singlet axial currents is secured [51]. The transformation rule is

$$\begin{aligned}\Delta w_{\rm S}(n,a=\mathrm{AR}) &= C_F\left\{2[S_1(n)]^2+2S_2(n)\right.\\ &\quad -S_1(n)\left(\frac{2}{n}-\frac{2}{n+1}+2\right)\\ &\quad \left.-2+\frac{1}{n}-\frac{1}{n+1}+\frac{2}{(n+1)^2}\right\},\end{aligned}\tag{3.32}$$

$$\Delta z(n,a=\mathrm{AR}) = \Delta\hat{z}(n,a=\mathrm{AR}) = 2N_f\frac{1}{n(n+1)}.\tag{3.33}$$

### 3.4 The DIS$_\gamma$ scheme

An interesting factorization scheme, which is called DIS$_\gamma$, was introduced some time ago in the NLO analysis of the unpolarized real photon structure function $F_2^\gamma(x,Q^2)$. Glück, Reya and Vogt [39] observed that, in the $\overline{\rm MS}$ scheme, the $\ln(1-x)$ term in the photonic coefficient function $C_2^\gamma(x)$ for $F_2^\gamma$, which becomes negative and divergent for $x\to 1$, drives the "point-like" part of $F_2^\gamma$ to large negative values as $x\to 1$, leading to a strong difference between the LO and the NLO results for $F_{2,\mathrm{point-like}}^\gamma$ in the large-$x$ region. They introduced the DIS$_\gamma$ scheme in which the photonic coefficient function $C_2^\gamma$, i.e., the direct-photon contribution to $F_2^\gamma$, is absorbed into the photonic quark distributions. It is noted that, for the real photon target, the structure function $F_2^\gamma$ is decomposed into a "point-like" and a "hadronic" part, the former being perturbatively calculable but the latter not. And beyond the LO both the "point-like" and the "hadronic" parts depend on the factorization scheme employed. A similar situation occurs in the polarized case, and the DIS$_\gamma$ scheme was applied to the NLO analysis for the spin-dependent structure function $g_1^\gamma(x,Q^2)$ of the real photon target by Stratmann and Vogelsang [18].

In the polarized version of the DIS$_\gamma$ scheme we take

$$\begin{aligned}&\Delta\, w_{\rm S}(n,\mathrm{DIS}_\gamma)\\ &\quad = \Delta w_{\rm NS}(n,\mathrm{DIS}_\gamma) = \Delta z(n,\mathrm{DIS}_\gamma) = 0,\end{aligned}\tag{3.34}$$

$$\begin{aligned}&\Delta\,\hat{z}(n,\mathrm{DIS}_\gamma)\\ &\quad = \frac{N_f}{4}\Delta B^n_{\gamma,\overline{\rm MS}}\\ &\quad = N_f\left\{-\frac{n-1}{n(n+1)}S_1(n)+\frac{3}{n}-\frac{4}{n+1}-\frac{1}{n^2}\right\},\end{aligned}\tag{3.35}$$

so that

$$\begin{aligned}\Delta B^n_{\gamma,\mathrm{DIS}_\gamma} &= \Delta B^n_{\gamma,\overline{\rm MS}}-\frac{4}{N_f}\Delta\hat{z}(n,\mathrm{DIS}_\gamma)\\ &= 0.\end{aligned}\tag{3.36}$$

Note that the relation à la (3.6) and (3.27) in the $\overline{\rm MS}$ and CI-like factorization schemes does not hold anymore in this scheme, i.e.,

$$\Delta B^n_{\gamma,\mathrm{DIS}_\gamma} \neq \frac{2}{N_f}\Delta B^n_{G,\mathrm{DIS}_\gamma}\left(=\frac{2}{N_f}\Delta B^n_{G,\overline{\rm MS}}\right).\tag{3.37}$$

For $n=1$, we have

$$\Delta\hat{z}(n=1,\mathrm{DIS}_\gamma)=0,\tag{3.38}$$

and thus, together with (3.34), we observe that as far as the first moments are concerned, DIS$_\gamma$ scheme gives the same results with $\overline{\rm MS}$. In other words, in the DIS$_\gamma$ scheme, both the QCD and QED axial anomaly effects are retained in the quark distributions.

With these preparations, we now examine the factorization-scheme dependence of the polarized parton distributions in the virtual photon. The two-loop anomalous dimensions of the spin-dependent operators and one-loop photon matrix elements of the hadronic operators in the $\overline{\rm MS}$ scheme are already known. Corresponding quantities in a particular scheme are obtained through the transformation rules given in (3.19). Inserting these quantities into the formulas given in Appendix A, we get the NLO predictions for the moments of polarized parton distributions in a particular factorization scheme.

### 3.5 Gluon distribution in the virtual photon

Let us start with the gluon distribution. We find that all the factorization schemes which we consider in this paper

[2] In fact, the author of [30] treated the $n=1$ moment of the gluon coefficient function differently from other moments. See also Appendix C.2 of [23]

predict the same behavior for the gluon distribution up to NLO:

$$\Delta G^\gamma(n,Q^2,P^2)|_a = \Delta G^\gamma(n,Q^2,P^2)|_{\overline{\rm MS}}, \tag{3.39}$$

where $a$ means the factorization schemes of CI, AB, OS, AR and DIS$_\gamma$. This can be seen from the direct calculation or from the notion that, up to NLO, $\Delta G^\gamma|_a$ satisfies the same evolution equation as $\Delta G^\gamma|_{\overline{\rm MS}}$ with the same initial condition at $Q^2 = P^2$, namely, $\Delta G^\gamma(n,P^2,P^2)|_a = \Delta G^\gamma(n,P^2,P^2)|_{\overline{\rm MS}} = 0$.

If we consider a more general factorization scheme in which the hadronic part of $Z_a^{-1}(n,Q^2)$ in (3.1) is replaced with a new one as follows:

$$\begin{pmatrix} 1-\frac{\alpha_{\rm s}}{2\pi}\Delta w_{\rm S} & -\frac{\alpha_{\rm s}}{2\pi}\Delta z \\ 0 & 1 \end{pmatrix} \Longrightarrow \begin{pmatrix} 1-\frac{\alpha_{\rm s}}{2\pi}\Delta w_{\rm S} & -\frac{\alpha_{\rm s}}{2\pi}\Delta z \\ -\frac{\alpha_{\rm s}}{2\pi}\Delta u & 1-\frac{\alpha_{\rm s}}{2\pi}\Delta v \end{pmatrix}, \tag{3.40}$$

then, in this new factorization scheme, the predicted gluon distribution is not the same as $\Delta G^\gamma(n,Q^2,P^2)|_{\overline{\rm MS}}$ in NLO. However, the first moment is found to be still the same. In other words, the first moment of the gluon distribution in the virtual photon, $\Delta G^\gamma(n=1,Q^2,P^2)$, is factorization-scheme independent up to NLO. This is due to the fact that the new terms, which appear by the inclusion of $\Delta u$ and $\Delta v$, will be proportional to $\Delta K_\psi^{0,n}$ and that $\Delta K_\psi^{0,n=1} = 0$. Also, the inclusion of $\Delta u$ and $\Delta v$ terms in $Z_a^{-1}$ does not modify the photon structure function $g_1^\gamma(x,Q^2,P^2)$ itself up to NLO, since the gluon coefficient function starts in the order $\alpha_{\rm s}$. Moreover, the quark distributions in the virtual photon do not change by the inclusion of $\Delta u$ and $\Delta v$ terms.

## 4 The $n = 1$ moments of the parton distributions

The first moments of the polarized parton distributions in the virtual photon are particularly interesting since they have relevance to the QCD and QED axial anomalies. The explicit expressions for the moments of $\Delta q_{\rm S}^\gamma$, $\Delta G^\gamma$, and $\Delta q_{\rm NS}^\gamma$ up to NLO are given in Appendix A. We take the $n \to 1$ limit in these expressions. Useful $n = 1$ moments of one- and two-loop anomalous dimensions, photon matrix elements, and coefficient functions both in the $\overline{\rm MS}$ and CI-like schemes are enumerated in Appendix B. As far as the first moments are concerned, the DIS$_\gamma$ scheme gives the same results as $\overline{\rm MS}$. Note that we have

$$\lambda_+^{n=1} = 0, \quad \lambda_-^{n=1} = -2\beta_0, \quad \lambda_{\rm NS}^{n=1} (= \Delta\gamma_{\rm NS}^{0,n=1}) = 0, \tag{4.1}$$

where $\lambda_\pm^{n=1}$ are eigenvalues of the one-loop hadronic anomalous dimension matrix $\Delta\gamma_{ij}^{0,n=1}$. The zero eigenvalues $\lambda_+^{n=1} = \lambda_{\rm NS}^{n=1} = 0$ correspond to the conservation of the axial-vector current at one-loop order.

### 4.1 The $n = 1$ moment of the gluon distribution

The expressions for the moments of the gluon distribution are given in Appendix A.2. In these expressions the factors

$$\frac{1}{\lambda_+^n}, \quad \frac{1}{2\beta_0+\lambda_-^n}, \quad \frac{1}{2\beta_0+\lambda_-^n-\lambda_+^n}, \tag{4.2}$$

may develop singularities at $n = 1$ and so we need to take a little care when we deal with them. Taking the limit of $n$ going to 1, we find

$$\begin{aligned} &\hat{L}_G^{+n} \to 0, \quad \hat{L}_G^{-n} \to \text{finite}, \\ &\hat{A}_G^{+n} \to \text{finite}, \quad \hat{B}_G^{+n} \to 0, \quad \hat{B}_G^{-n} \to \text{finite}, \\ &\hat{A}_G^{-n} \to 72\langle e^2\rangle N_f C_F. \end{aligned} \tag{4.3}$$

The terms proportional to $\hat{L}_G^{-n}$, $\hat{B}_G^{-n}$, and $\hat{A}_G^{+n}$ all vanish in the $n = 1$ limit, since they are multiplied by the following vanishing factors:

$$\left\{1-\left[\frac{\alpha_{\rm s}(Q^2)}{\alpha_{\rm s}(P^2)}\right]^{\lambda_-^n/2\beta_0+1}\right\}, \quad \left\{1-\left[\frac{\alpha_{\rm s}(Q^2)}{\alpha_{\rm s}(P^2)}\right]^{\lambda_+^n/2\beta_0}\right\}. \tag{4.4}$$

The only exception is the term proportional to $\hat{A}_G^{-n}$. We find for $n \to 1$

$$\begin{aligned} &\hat{A}_G^{-n}\left\{1-\left[\frac{\alpha_{\rm s}(Q^2)}{\alpha_{\rm s}(P^2)}\right]^{\lambda_-^n/2\beta_0}\right\} \\ &\quad \to 72\langle e^2\rangle N_f C_F \frac{\alpha_{\rm s}(Q^2)-\alpha_{\rm s}(P^2)}{\alpha_{\rm s}(Q^2)}. \end{aligned} \tag{4.5}$$

Thus we obtain

$$\Delta G^\gamma(n=1,Q^2,P^2) = \frac{12\alpha}{\pi\beta_0}\langle e^2\rangle N_f \frac{\alpha_{\rm s}(Q^2)-\alpha_{\rm s}(P^2)}{\alpha_{\rm s}(Q^2)} \tag{4.6}$$

for the first moment of the gluon distribution in the virtual photon. It should be emphasized that this result is factorization-scheme independent.

### 4.2 The $n = 1$ moment of the quark distributions

The expressions for the moments of the quark distributions are given in Appendix A.1 and A.3. In all the factorization schemes under study, i.e., the $\overline{\rm MS}$, DIS$_\gamma$ and the CI-like schemes, we find for $n \to 1$

$$\begin{aligned} &\hat{L}_{\rm S}^{+n} \to 0, \quad \hat{L}_{\rm S}^{-n} \to 0, \quad \hat{L}_{\rm NS}^{n} \to 0, \\ &\hat{A}_{\rm S}^{+n} \to \text{finite}, \quad \hat{A}_{\rm S}^{-n} \to 0, \quad \hat{A}_{\rm NS}^{n} \to \text{finite}, \\ &\hat{B}_{\rm S}^{+n} \to 0, \quad \hat{B}_{\rm S}^{-n} \to \text{finite}, \quad \hat{B}_{\rm NS}^{n} \to 0. \end{aligned} \tag{4.7}$$

The terms proportional to $\hat{A}_{\rm S}^{+n}$ and $\hat{B}_{\rm S}^{-n}$ are multiplied by the vanishing factors in (4.4), and the $\hat{A}_{\rm NS}^n$ term is multiplied by

$$\left\{1-\left[\frac{\alpha_{\rm s}(Q^2)}{\alpha_{\rm s}(P^2)}\right]^{\lambda_{\rm NS}^n/2\beta_0}\right\}, \tag{4.8}$$

and, therefore, the $\hat{L}_{\rm S}^{+n}$, $\hat{L}_{\rm S}^{-n}$, $\hat{L}_{\rm NS}^{n}$, $\hat{A}_{\rm S}^{+n}$, $\hat{A}_{\rm S}^{-n}$, $\hat{A}_{\rm NS}^{n}$, $\hat{B}_{\rm S}^{+n}$, $\hat{B}_{\rm S}^{-n}$, and $\hat{B}_{\rm NS}^{n}$ terms in (A.1) and (A.17) all vanish in the $n = 1$ limit. Then the first moments of the quark distributions are given by

$$\Delta q_{\rm S}^{\gamma}(n=1,Q^2,P^2) = \frac{\alpha}{8\pi\beta_0}\hat{C}_{\rm S}^{n=1} = \frac{\alpha}{4\pi}\Delta A_{\psi}^{n=1}, \quad (4.9)$$

$$\Delta q_{\rm NS}^{\gamma}(n=1,Q^2,P^2) = \frac{\alpha}{8\pi\beta_0}\hat{C}_{\rm NS}^{n=1} = \frac{\alpha}{4\pi}\Delta A_{\rm NS}^{n=1}. \quad (4.10)$$

We now see that scheme dependence for the first moments of the quark distributions is coming from the photon matrix elements $\Delta A_{\psi}^{n}$ and $\Delta A_{\rm NS}^{n}$.

In the case of CI-like factorization schemes, $a = {\rm CI}$, AB, OS, AR, we have

$$\begin{aligned}&\Delta w(n=1,a) = 0,\\ &\Delta z(n=1,a) = \Delta\hat{z}(n=1,a) = N_f,\\ &\qquad\qquad \text{for } a = {\rm CI, AB, OS, AR}. \end{aligned} \quad (4.11)$$

We find from (3.22) and (3.25) that these schemes give

$$\Delta A_{\psi,a}^{n=1} = \Delta A_{{\rm NS},a}^{n=1} = 0. \quad (4.12)$$

This leads to an interesting result: The first moment of spin-dependent quark distributions in the virtual photon vanish in NLO for $a = {\rm CI, AB, OS, AR}$. We have

$$\Delta q_{\rm S}^{\gamma}(n=1,Q^2,P^2)|_a = \Delta q_{\rm NS}^{\gamma}(n=1,Q^2,P^2)|_a = 0. \quad (4.13)$$

The vanishing first moments imply that the axial anomaly effects do not reside in the quark distributions. In these CI-like schemes, the QCD and QED axial anomalies are transfered to the gluon and photon coefficient functions, respectively, and their first moments do not vanish. Indeed we obtain from (3.1) and (3.8)

$$\Delta C_{G,a}^{\gamma,n=1} = -\langle e^2\rangle\frac{\alpha_{\rm s}(Q^2)}{2\pi}N_f, \quad (4.14)$$

$$\Delta C_{\gamma,a}^{\gamma,n=1} = -\frac{3\alpha}{\pi}\langle e^4\rangle N_f\left(1-\frac{\alpha_{\rm s}(Q^2)}{\pi}\right), \quad \text{for } a = {\rm CI, AB, OS, AR}, \quad (4.15)$$

where we have used [45,52,23]

$$\frac{1}{\langle e^2\rangle}\Delta C_{\rm S}^{\gamma,n=1}|_{\overline{\rm MS}} = \Delta C_{\rm NS}^{\gamma,n=1}|_{\overline{\rm MS}} = 1-\frac{\alpha_{\rm s}}{\pi}+\mathcal{O}(\alpha_s^2), \quad (4.16)$$

$$\Delta C_{\gamma}^{\gamma,n=1}|_{\overline{\rm MS}} = 0+\mathcal{O}(\alpha\alpha_s^2). \quad (4.17)$$

On the other hand, in the $\overline{\rm MS}$ (and also in the ${\rm DIS}_{\gamma}$) case we obtain from (2.5)

$$\Delta A_{\psi,\overline{\rm MS}}^{n=1} = -12\langle e^2\rangle N_f, \quad (4.18)$$

$$\Delta A_{{\rm NS},\overline{\rm MS}}^{n=1} = -12(\langle e^4\rangle - \langle e^2\rangle^2)N_f, \quad (4.19)$$

and thus $\Delta q_{\rm S}^{\gamma,n=1}|_{\overline{\rm MS}}$ and $\Delta q_{\rm NS}^{\gamma,n=1}|_{\overline{\rm MS}}$ are non-zero constant. Actually we can go one step further to in the order of the $\alpha_{\rm s}$ QCD corrections. This is due to the fact that, in the $\overline{\rm MS}$ scheme, the parton distribution $\Delta\boldsymbol{q}^{\gamma}(n=1)|_{\overline{\rm MS}} = (\Delta q_{\rm S}^{\gamma}, \Delta G^{\gamma}, \Delta q_{\rm NS}^{\gamma})|_{\overline{\rm MS}}$ satisfies a homogeneous differential equation without inhomogeneous LO and NLO $\Delta K$ terms. Indeed, we find

$$\begin{aligned}&\Delta q_{\rm S}^{\gamma}(n=1,Q^2,P^2)|_{\overline{\rm MS}}\\ &= \left[-\frac{\alpha}{\pi}3\langle e^2\rangle N_f\right]\left\{1-\frac{2}{\beta_0}\frac{\alpha_{\rm s}(P^2)-\alpha_{\rm s}(Q^2)}{\pi}N_f\right\}, \end{aligned} \quad (4.20)$$

$$\begin{aligned}&\Delta q_{\rm NS}^{\gamma}(n=1,Q^2,P^2)|_{\overline{\rm MS}}\\ &= \left[-\frac{\alpha}{\pi}3(\langle e^4\rangle - \langle e^2\rangle^2)N_f\right]\left\{1+\mathcal{O}(\alpha_{\rm s}^2)\right\}, \end{aligned} \quad (4.21)$$

the derivation of which is shown in Appendix C. In the $\overline{\rm MS}$ scheme, the axial anomaly effects are retained in the quark distributions. The factors $\left[-(\alpha/\pi)3\langle e^2\rangle N_f\right]$ and $[-(\alpha/\pi)3(\langle e^4\rangle - \langle e^2\rangle^2)N_f]$ are related to the QED axial anomaly and a term $(2/\beta_0)(\alpha_{\rm s}(P^2)-\alpha_{\rm s}(Q^2))/\pi N_f$ in $\Delta q_{\rm S}^{\gamma,n=1}|_{\overline{\rm MS}}$ is coming from the QCD axial anomaly.

### 4.3 The $n = 1$ moment of $g_1^{\gamma}(x, Q^2, P^2)$

The polarized structure function $g_1^{\gamma}(x,Q^2,P^2)$ of the virtual photon satisfies the following sum rule [20,23]:

$$\begin{aligned}&\int_0^1 {\rm d}x g_1^{\gamma}(x,Q^2,P^2)\\ &= -\frac{3\alpha}{\pi}\langle e^4\rangle N_f\left(1-\frac{\alpha_{\rm s}(Q^2)}{\pi}\right)\\ &\quad +\frac{6\alpha}{\pi\beta_0}[\langle e^2\rangle N_f]^2\frac{\alpha_{\rm s}(P^2)-\alpha_{\rm s}(Q^2)}{\pi}+\mathcal{O}(\alpha_{\rm s}^2). \end{aligned} \quad (4.22)$$

This sum rule is of course factorization-scheme independent. Now we examine how the scheme-dependent parton distributions contribute to this sum rule. In the CI-like schemes ($a = {\rm CI, AB, OS, AR}$), the first moment of the quark distributions vanish in NLO, and thus the contribution to the sum rule comes from the gluon and photon distributions. Equations (4.6) and (4.15) show that

$$\Delta C_{G,a}^{\gamma,n=1}\Delta G^{\gamma}(n=1,Q^2,P^2)|_a + \Delta C_{\gamma,a}^{\gamma,n=1} \quad (4.23)$$

leads to the result (4.22). On the other hand, in the $\overline{\rm MS}$ scheme (and also in ${\rm DIS}_{\gamma}$), the one-loop gluon and photon coefficient functions vanish, $\Delta B_{G,\overline{\rm MS}}^{n=1} = \Delta B_{\gamma,\overline{\rm MS}}^{n=1} = 0$ and, therefore, the sum rule is derived from the quark contributions. Indeed we find from (4.16), (4.20)–(4.21)

$$\begin{aligned}&\Delta C_{{\rm S},\overline{\rm MS}}^{\gamma,n=1}\Delta q_{\rm S}^{\gamma}(n=1,Q^2,P^2)|_{\overline{\rm MS}}\\ &\quad +\Delta C_{{\rm NS},\overline{\rm MS}}^{\gamma,n=1}\Delta q_{\rm NS}^{\gamma}(n=1,Q^2,P^2)|_{\overline{\rm MS}} \end{aligned} \quad (4.24)$$

leads to the same result.

It is interesting to note that the sum rule (4.22) is the consequence of the QCD and QED axial anomalies and that in the CI-like schemes the anomaly effect resides in the gluon contribution while in $\overline{\rm MS}$, it is in the quark

contributions. Furthermore, the first term of the sum rule (4.22) is coming from the QED axial anomaly and the second one is from the QCD axial anomaly[3].

## 5 Behaviors of parton distributions near $x = 1$

The behaviors of the parton distributions near $x = 1$ are governed by the large-$n$ limit of those moments. In the leading order, parton distributions are factorization-scheme independent. For large $n$, $\Delta q_{\rm S}^{\gamma}(n,Q^2,P^2)|_{\rm LO}$ and $\Delta q_{\rm NS}^{\gamma}(n,Q^2,P^2)|_{\rm LO}$ behave as $1/(n\ln n)$, while $\Delta G^{\gamma}(n,Q^2,P^2)|_{\rm LO} \propto 1/(n\ln n)^2$. Thus in $x$ space, the parton distributions vanish for $x \to 1$. In fact, we find

$$\Delta q_{\rm S}^{\gamma}(x,Q^2,P^2)|_{\rm LO} \approx \frac{\alpha}{4\pi}\frac{4\pi}{\alpha_{\rm s}(Q^2)}N_f\langle e^2\rangle\frac{9}{4}\frac{-1}{\ln(1-x)}, \tag{5.1}$$

$$\Delta G^{\gamma}(x,Q^2,P^2)|_{\rm LO} \approx \frac{\alpha}{4\pi}\frac{4\pi}{\alpha_{\rm s}(Q^2)}N_f\langle e^2\rangle\frac{1}{2}\frac{-\ln x}{\ln^2(1-x)}. \tag{5.2}$$

The behaviors of $\Delta q_{\rm NS}^{\gamma}(x,Q^2,P^2)$ for $x \to 1$, both in LO and NLO, are always given by the corresponding expressions for $\Delta q_{\rm S}^{\gamma}(x,Q^2,P^2)$ with replacement of the charge factor $\langle e^2\rangle$ with $(\langle e^4\rangle - \langle e^2\rangle^2)$.

In the $\overline{\rm MS}$ scheme, the moments of the NLO parton distributions are written in the large-$n$ limit as

$$\Delta q_{\rm S}^{\gamma}(n,Q^2,P^2)|_{\rm NLO,\overline{MS}} \longrightarrow \frac{\alpha}{4\pi}N_f\langle e^2\rangle 6\frac{\ln n}{n}, \tag{5.3}$$

$$\Delta G^{\gamma}(n,Q^2,P^2)|_{\rm NLO,\overline{MS}} \longrightarrow \frac{\alpha}{4\pi}N_f\langle e^2\rangle 3\frac{1}{n^2}. \tag{5.4}$$

So we have near $x = 1$

$$\Delta q_{\rm S}^{\gamma}(x,Q^2,P^2)|_{\rm NLO,\overline{MS}} \approx \frac{\alpha}{4\pi}N_f\langle e^2\rangle 6[-\ln(1-x)], \tag{5.5}$$

$$\Delta G^{\gamma}(x,Q^2,P^2)|_{\rm NLO,\overline{MS}} \approx \frac{\alpha}{4\pi}N_f\langle e^2\rangle 3[-\ln x]. \tag{5.6}$$

It is remarkable that, in the $\overline{\rm MS}$ scheme, the quark parton distributions, $\Delta q_{\rm S}^{\gamma}(x)|_{\rm NLO,\overline{MS}}$ and $\Delta q_{\rm NS}^{\gamma}(x)|_{\rm NLO,\overline{MS}}$, positively diverge as $[-\ln(1-x)]$ for $x \to 1$. Recall that $\Delta G^{\gamma}(x,Q^2,P^2)|_{\rm NLO}$ is the same among the schemes which we consider in this paper. The NLO quark distributions in the CI, AB, AR and DIS$_\gamma$ schemes also diverge as $x \to 1$, since their moments behave as $\ln n/n$ in the large-$n$ limit. We find for large $x$

$$\Delta q_{\rm S}^{\gamma}(x,Q^2,P^2)|_{\rm NLO,CI} \approx \frac{\alpha}{4\pi}N_f\langle e^2\rangle 6[-\ln(1-x)], \tag{5.7}$$

$$\Delta q_{\rm S}^{\gamma}(x,Q^2,P^2)|_{\rm NLO,AB} \approx \frac{\alpha}{4\pi}N_f\langle e^2\rangle 6[-\ln(1-x)+2], \tag{5.8}$$

$$\Delta q_{\rm S}^{\gamma}(x,Q^2,P^2)|_{\rm NLO,AR} \approx \frac{\alpha}{4\pi}N_f\langle e^2\rangle 18[-\ln(1-x)], \tag{5.9}$$

$$\Delta q_{\rm S}^{\gamma}(x,Q^2,P^2)|_{\rm NLO,DIS_\gamma} \approx \frac{\alpha}{4\pi}N_f\langle e^2\rangle 6\ln(1-x). \tag{5.10}$$

It is noted that $\Delta q_{\rm S}^{\gamma}(x,Q^2,P^2)|_{\rm NLO,DIS_\gamma}$ negatively diverges as $x \to 1$. This is due to the fact that the photonic coefficient function $\Delta C_{\gamma}^{\gamma}(x)$, which in $\overline{\rm MS}$ becomes negative and divergent for $x \to 1$, is absorbed into the quark distributions in the DIS$_\gamma$ scheme.

On the other hand, the OS scheme gives quite different behaviors near $x = 1$ for the quark distributions. Since the typical two-loop anomalous dimensions in the OS scheme behave in the large-$n$ limit as

$$\Delta\gamma_{\rm NS,OS}^{(1),n} \sim \Delta\gamma_{qq,\rm OS}^{(1),n} \propto \ln^2 n, \quad \Delta K_{\rm S,OS}^{(1),n} \propto \frac{\ln n}{n}, \tag{5.11}$$

while in the $\overline{\rm MS}$ scheme

$$\Delta\gamma_{\rm NS,\overline{MS}}^{(1),n} \sim \Delta\gamma_{qq,\overline{\rm MS}}^{(1),n} \propto \ln n, \quad \Delta K_{\rm S,\overline{MS}}^{(1),n} \propto \frac{\ln^2 n}{n}, \tag{5.12}$$

we find that the moment of $\Delta q_{\rm S}^{\gamma}(n,Q^2,P^2)|_{\rm NLO}$ in the OS scheme is expressed in the large-$n$ limit as

$$\Delta q_{\rm S}^{\gamma}(n,Q^2,P^2)|_{\rm NLO,OS} \longrightarrow \frac{\alpha}{4\pi}N_f\langle e^2\rangle\left[\frac{69}{8}+\frac{3}{4}N_f\right]\frac{1}{n}. \tag{5.13}$$

In $x$ space, $\Delta q_{\rm S}^{\gamma}(x,Q^2,P^2)|_{\rm NLO,OS}$ does not diverge for $x \to 1$ but approaches a constant value:

$$\Delta q_{\rm S}^{\gamma}(x,Q^2,P^2)|_{\rm NLO,OS} \longrightarrow \frac{\alpha}{4\pi}N_f\langle e^2\rangle\left[\frac{69}{8}+\frac{3}{4}N_f\right]. \tag{5.14}$$

Therefore, as far as the large-$x$ behaviors of the quark distributions, and gluon and photon coefficient functions (see (5.18)–(5.19) below) are concerned, the OS scheme is more appropriate than other schemes in the sense that they remain finite. Also the quark coefficient function in the OS scheme has a milder divergence for $x \to 1$ than those predicted in other schemes (see (5.17)).

Before ending this section, we now show that, as $x \to 1$, the polarized virtual photon structure function $g_1^{\gamma}(x,Q^2,P^2)$ approaches a constant value:

$$\kappa = \frac{\alpha}{4\pi}N_f\langle e^4\rangle\left[-\frac{51}{8}+\frac{3}{4}N_f\right] \tag{5.15}$$

in NLO. This result is, of course, factorization-scheme independent. It is interesting to note that the constant value $\kappa$ coincides exactly with the one given in (4.39) of [53], which was derived as the large-$n$ limit of the moment of the NLO term $b_2(x)$ for the unpolarized structure function $F_2^{\gamma}$ [1]. In the leading order, (5.1) tells us that

$$g_1^{\gamma}(x,Q^2,P^2)|_{\rm LO} = \langle e^2\rangle\Delta q_{\rm S}^{\gamma}(x,Q^2,P^2)|_{\rm LO} + \Delta q_{\rm NS}^{\gamma}(x,Q^2,P^2)|_{\rm LO} \longrightarrow \frac{\alpha}{4\pi}\frac{4\pi}{\alpha_{\rm s}(Q^2)}N_f\langle e^4\rangle\frac{9}{4}\frac{-1}{\ln(1-x)}, \tag{5.16}$$

[3] This notion was first pointed out by the authors of [20]

and thus $g_1^\gamma(x,Q^2,P^2)|_{\rm LO}$ vanishes as $x\to 1$.

In order to analyze the large $x$-behavior of the next-leading order, $g_1^\gamma(x,Q^2,P^2)|_{\rm NLO}$, we need information on the coefficient functions. Note that $\Delta B_{\rm NS}^n|_a = \Delta B_{\rm S}^n|_a$. They behave, for $x\to 1$, as

$$\Delta B_{\rm S}(x)|_a \longrightarrow \begin{cases} 2C_F\left[\dfrac{2\ln(1-x)}{1-x}\right]_+ & \text{for } a=\overline{\rm MS},{\rm CI},{\rm AB},{\rm DIS}_\gamma,\\ -2C_F\left[\dfrac{2\ln(1-x)}{1-x}\right]_+ & \text{for } a={\rm AR},\\ 3C_F\dfrac{-1}{(1-x)_+} & \text{for } a={\rm OS}, \end{cases} \tag{5.17}$$

$$\Delta B_G(x)|_a \longrightarrow \begin{cases} 2N_f\ln(1-x) & \text{for } a=\overline{\rm MS},{\rm CI},{\rm AB},{\rm AR},{\rm DIS}_\gamma,\\ -4N_f & \text{for } a={\rm OS}, \end{cases} \tag{5.18}$$

$$\Delta C(x)_\gamma^\gamma|_a \longrightarrow \begin{cases} \dfrac{\alpha}{4\pi}\langle e^4\rangle 12N_f\ln(1-x) & \text{for } a=\overline{\rm MS},{\rm CI},{\rm AB},{\rm AR}\ ,\\ -\dfrac{\alpha}{4\pi}\langle e^4\rangle 24N_f & \text{for } a={\rm OS},\\ 0 & \text{for } a={\rm DIS}_\gamma. \end{cases} \tag{5.19}$$

The coefficient functions $\Delta B_{\rm S}(x)$ and $\Delta B_G(x)$ are the same as the ones that appear in the polarized nucleon structure function $g_1(x,Q^2)$. $\Delta B_{\rm S}(x)$ in all schemes considered here diverges as $x\to 1$, but the OS scheme gives a milder divergence for $\Delta B_{\rm S}(x)$ than the other schemes. Also note that $\Delta B_G(x)|_{\rm OS}$ remains finite as $x\to 1$, but the $\Delta B_G(x)$ in other schemes negatively diverge.

Let us write $g_1^\gamma(x,Q^2,P^2)|_{\rm NLO}$ in terms of the partonic contributions as follows:

$$g_1^\gamma(x,Q^2,P^2)|_{\rm NLO} = g_1^\gamma(x)|_{\rm NLO}^{\rm quark} + g_1^\gamma(x)|_{\rm NLO}^{\rm gluon} + \Delta C_\gamma^\gamma(x), \tag{5.20}$$

where

$$\begin{aligned} g_1^\gamma(x)|_{\rm NLO}^{\rm quark} &\equiv \langle e^2\rangle \Delta q_{\rm S}^\gamma(x,Q^2,P^2)|_{\rm NLO} + \Delta q_{\rm NS}^\gamma(x,Q^2,P^2)|_{\rm NLO}\\ &+\langle e^2\rangle \frac{\alpha_{\rm s}(Q^2)}{4\pi}\Delta B_{\rm S}(x)\otimes \Delta q_{\rm S}^\gamma(x,Q^2,P^2)|_{\rm LO}\\ &+\frac{\alpha_{\rm s}(Q^2)}{4\pi}\Delta B_{\rm NS}(x)\otimes \Delta q_{\rm NS}^\gamma(x,Q^2,P^2)|_{\rm LO}, \end{aligned} \tag{5.21}$$

$$g_1^\gamma(x)|_{\rm NLO}^{\rm gluon} \equiv \langle e^2\rangle \frac{\alpha_{\rm s}(Q^2)}{4\pi}\Delta B_G(x)\otimes \Delta G^\gamma(x,Q^2,P^2)|_{\rm LO}. \tag{5.22}$$

Then we find, for $x\to 1$,

$$g_1^\gamma(x)|_{\rm NLO}^{\rm quark} \longrightarrow \begin{cases} -\dfrac{\alpha}{4\pi}\langle e^4\rangle 12N_f\ln(1-x) & \text{for } a=\overline{\rm MS},{\rm CI},{\rm AB},{\rm AR},\\ \dfrac{\alpha}{4\pi}\langle e^4\rangle N_f\left[\dfrac{141}{8}+\dfrac{3}{4}N_f\right] & \text{for } a={\rm OS},\\ \dfrac{\alpha}{4\pi}\langle e^4\rangle N_f\left[-\dfrac{51}{8}+\dfrac{3}{4}N_f\right] & \text{for } a={\rm DIS}_\gamma. \end{cases} \tag{5.23}$$

The NLO gluon contribution $g_1^\gamma(x,Q^2,P^2)|_{\rm NLO}^{\rm gluon}$ vanishes faster than $(\ln x)^2$ in any scheme under consideration. As for the NLO quark contribution, $g_1^\gamma(x,Q^2,P^2)|_{\rm NLO}^{\rm quark}$ in the $\overline{\rm MS}$, CI, AB, AR schemes diverges as $[-\ln(1-x)]$ for $x\to 1$. However, (5.19) shows that the one-loop photon coefficient function $\Delta C_\gamma^\gamma(x)$ in these schemes also diverges as $[-\ln(1-x)]$ with opposite sign, and the sum becomes finite. On the other hand, in the OS scheme, we observe from (5.23) and (5.19) that both the quark contribution and the photon coefficient function remain finite as $x\to 1$, and it is easily seen that the sum

$$g_1^\gamma(x)|_{\rm NLO,OS}^{\rm quark} + \Delta C(x)_{\gamma,{\rm OS}}^\gamma \tag{5.24}$$

approaches the constant value $\kappa$ given in (5.15). In the ${\rm DIS}_\gamma$ scheme, the NLO quark contribution $g_1^\gamma(x)|_{\rm NLO,DIS_\gamma}^{\rm quark}$ reaches the finite value $\kappa$ as $x\to 1$, since $\Delta C(x)_{\gamma,{\rm DIS}_\gamma}^\gamma \equiv 0$. In fact, as we see from (5.21), $g_1^\gamma(x)|_{\rm NLO}^{\rm quark}$ is made up of two parts, one from $\Delta q_{\rm S}^\gamma(x,Q^2,P^2)|_{\rm NLO}$ and the other from $\Delta B_{\rm S}(x)\otimes \Delta q_{\rm S}^\gamma(x,Q^2,P^2)|_{\rm LO}$, plus their non-singlet quark counterparts. In ${\rm DIS}_\gamma$, both contributions diverge as $x\to 1$, but with opposite sign, and the sum remains finite.

The constant value $\kappa$ in (5.15) is negative unless $N_f \geq 9$. Consequently, it seems superficially that QCD with eight flavors or less predicts that the structure function $g_1^\gamma(x,Q^2,P^2)$ turns out to be negative for $x$ very close to 1, since the leading term $g_1^\gamma(x,Q^2,P^2)|_{\rm LO}$ vanishes as $x\to 1$. But the fact is that $x$ cannot reach exactly one. The constraint $(p+q)^2\geq 0$ gives

$$x \leq x_{\rm max} = \frac{Q^2}{Q^2+P^2}, \tag{5.25}$$

and we find

$$g_1^\gamma(x=x_{\rm max},Q^2,P^2)|_{\rm LO} > \frac{\alpha}{4\pi}N_f\langle e^4\rangle\frac{3}{C_F}\beta_0, \tag{5.26}$$

and the sum $g_1^\gamma(x=x_{\rm max},Q^2,P^2)|_{\rm LO+NLO}$ is indeed positive.

## 6 Numerical analysis

The parton distribution functions are recovered from the moments by the inverse Mellin transformation. In Fig. 2 we plot the factorization-scheme dependence of the singlet quark distribution $\Delta q_{\rm S}^\gamma(x,Q^2,P^2)$ beyond the LO in units of $(3N_f\langle e^2\rangle\alpha/\pi)\ln(Q^2/P^2)$. We have taken $N_f=3$, $Q^2 = 30\,{\rm GeV}^2$, $P^2 = 1\,{\rm GeV}^2$, and the QCD scale parameter

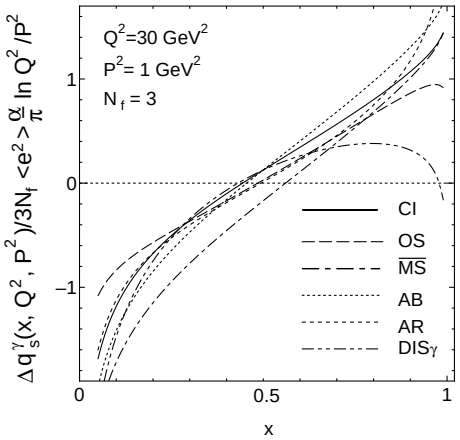


**Fig. 2.** Factorization-scheme dependence of the polarized singlet quark distribution $\Delta q_{\rm S}^{\gamma}(x,Q^2,P^2)$ up to NLO in units of $(3N_f\langle e^2\rangle\alpha/\pi)\ln(Q^2/P^2)$ with $N_f=3$, $Q^2=30\,{\rm GeV}^2$, $P^2=1\,{\rm GeV}^2$, and the QCD scale parameter $\Lambda=0.2\,{\rm GeV}$, for $\overline{\rm MS}$ (dash-dotted line), CI (solid line), AB (short-dashed line), OS (long-dashed line), AR (dashed line) and DIS$_\gamma$ (dash-2dotted line) schemes

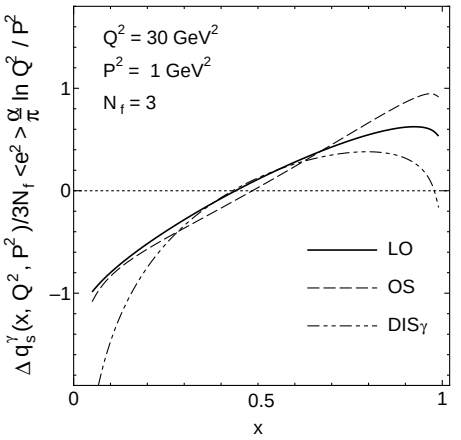


**Fig. 3.** The polarized singlet quark distribution $\Delta q_{\rm S}^{\gamma}(x,Q^2,P^2)$ up to NLO predicted by the OS and DIS$_\gamma$ schemes in units of $(3N_f\langle e^2\rangle\alpha/\pi)\ln(Q^2/P^2)$ for $N_f=3$, $Q^2=30\,{\rm GeV}^2$, $P^2=1\,{\rm GeV}^2$, and $\Lambda=0.2\,{\rm GeV}$, together with the LO result

$\Lambda=0.2\,{\rm GeV}$. All four CI-like (i.e., CI, AB, OS and AR) curves cross the $x$-axis nearly at the same point, just below $x=0.5$, while the $\overline{\rm MS}$ curve crosses above $x=0.5$. This is understandable since we saw from (4.13) and (4.20) that the first moment of $\Delta q_{\rm S}^{\gamma}$ vanishes in the CI-like schemes while it is negative in the $\overline{\rm MS}$ scheme. The DIS$_\gamma$ curve crosses the $x$-axis below $x=0.5$, though the first moment of $\Delta q_{\rm S}^{\gamma}|_{\rm DIS_\gamma}$ is negative, taking the same value as the one in the $\overline{\rm MS}$ scheme. Comparing the DIS$_\gamma$ curve at large $x$ with the $\overline{\rm MS}$ one, we will see that the rapid dropping of the DIS$_\gamma$ curve as $x\to1$ drives the crossing point below $x=0.5$.

As $x\to1$, we observe that the $\overline{\rm MS}$, CI, AB, and AR curves continue to increase. In fact, we see that the $\overline{\rm MS}$ and CI curves tend to merge, the AB curve comes above those two curves, and the AR curve diverges more rapidly than the other three. On the other hand, the OS and DIS$_\gamma$ curves start to drop at large $x$. The OS curve continues to increase till near $x=1$, and then starts to drop to reach a finite positive value. The DIS$_\gamma$ curve reaches a maximum at $x\approx0.8$ and drops to negative values. These behaviors are inferred from (5.5), (5.7)–(5.10) and (5.14).

Concerning the non-singlet quark distribution $\Delta q_{\rm NS}^{\gamma}(x,Q^2,P^2)$, we find that when we take into account the charge factors, it falls on the singlet quark distribution in almost the whole $x$ region; namely the two "normalized" distributions $\Delta\widetilde{q}_{\rm S}^{\gamma}\equiv\Delta q_{\rm S}^{\gamma}/\langle e^2\rangle$ and $\Delta\widetilde{q}_{\rm NS}^{\gamma}\equiv\Delta q_{\rm NS}^{\gamma}/(\langle e^4\rangle-\langle e^2\rangle^2)$ mostly overlap except at the very small $x$ region. This situation is the same in all factorization schemes we have studied in this paper. This is attributable to the fact that once the charge factors are taken into account, the evolution equations for both $\Delta\widetilde{q}_{\rm S}^{\gamma}$ and $\Delta\widetilde{q}_{\rm NS}^{\gamma}$ have the same inhomogeneous LO and NLO $\Delta K$ terms and the same initial conditions at $Q^2=P^2$ (see (3.20)).

In Fig. 3 we plot again the OS and DIS$_\gamma$ predictions for $\Delta q_{\rm S}^{\gamma}(x,Q^2,P^2)$ together with the LO result. The motivation to introduce the DIS$_\gamma$ scheme into the analysis of the unpolarized (polarized) real photon structure function $F_2^{\gamma}$ ($g_1^{\gamma}$) was to reduce the discrepancies at the large-$x$ region between the LO and the NLO results for the "point-like" part of $F_2^{\gamma}$ ($g_1^{\gamma}$). When applied to the polarized virtual photon case, it is seen from Figs. 2 and 3 that the DIS$_\gamma$ scheme gives a better behavior for $\Delta q_{\rm S}^{\gamma}(x,Q^2,P^2)$ at large $x$ than $\overline{\rm MS}$ in the sense that the DIS$_\gamma$ curve is closer to the LO result. However, we observe that absorbing the photonic coefficient function $\Delta C_{\gamma}^{\gamma}$ into the quark distributions in the DIS$_\gamma$ scheme has too much effect on their large-$x$ behaviors: The DIS$_\gamma$ curve for $\Delta q_{\rm S}^{\gamma}(x,Q^2,P^2)$ goes under the LO one at $x\approx0.6$ and the difference between the two grows as $x\to1$. In fact, the DIS$_\gamma$ curve drops to negative values near at $x=1$.

From the viewpoint of "perturbative stabilities" we find that the OS curve shows a more appropriate behavior than the other ones. We see from Fig. 3 that the differences between the OS and LO curves are very small for the range $0.05<x<0.7$. And the OS curve turns out to lie above the LO for $x>0.7$.

Figure 4 shows the $Q^2$-dependence of $\Delta q_{\rm S}^{\gamma}(x,Q^2,P^2)$ in the OS scheme in units of $(3N_f\langle e^2\rangle\alpha/\pi)\ln(Q^2/P^2)$. Three curves with $Q^2=30,50$ and $100\,{\rm GeV}^2$ almost overlap in the whole $x$ region except in the vicinity of $x=1$. We see from Fig. 4 that, in the OS scheme, $\Delta q_{\rm S}^{\gamma}$ beyond the LO behaves approximately as the one obtained from the box (tree) diagram calculation,

$$\Delta q_{\rm S}^{\gamma({\rm box})}(x,Q^2,P^2)=(2x-1)3N_f\langle e^2\rangle\frac{\alpha}{\pi}\ln\frac{Q^2}{P^2}. \quad (6.1)$$

The gluon distribution $\Delta G^{\gamma}(x,Q^2,P^2)$ beyond the LO is shown in Fig. 5 in units of $(3N_f\langle e^2\rangle\alpha/\pi)\ln(Q^2/P^2)$, with three different $Q^2$ values. Recall that every scheme considered in this paper predicts the same behavior for the gluon distribution up to NLO. We do not see much differences in the three curves with different $Q^2$. This means that $\Delta G^{\gamma}$ is approximately proportional to $\ln(Q^2/P^2)$.

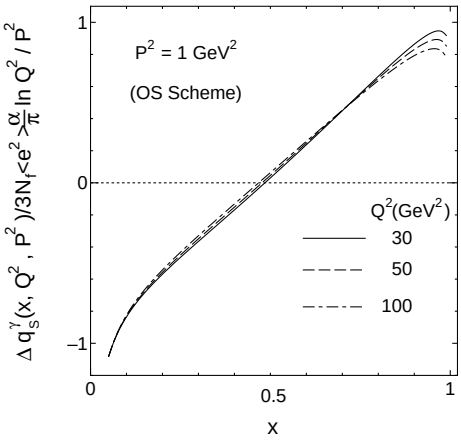


**Fig. 4.** The polarized singlet quark distribution $\Delta q_S^\gamma(x, Q^2, P^2)$ up to NLO in the OS scheme in units of $(3N_f\langle e^2\rangle\alpha/\pi)\ln(Q^2/P^2)$ with three different $Q^2$ values, for $N_f = 3$, $P^2 = 1\,\mathrm{GeV}^2$, and $\Lambda = 0.2\,\mathrm{GeV}$

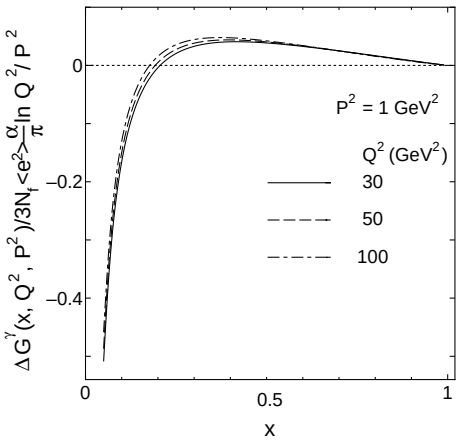


**Fig. 5.** The polarized gluon distribution $\Delta G^\gamma(x, Q^2, P^2)$ beyond the LO in units of $(3N_f\langle e^2\rangle\alpha/\pi)\ln(Q^2/P^2)$ with three different $Q^2$ values, for $N_f = 3$, $P^2 = 1\,\mathrm{GeV}^2$, and $\Lambda = 0.2\,\mathrm{GeV}$

But, compared with the quark distributions, $\Delta G^\gamma$ is very small in absolute value except in the small-$x$ region.

In Fig. 6 we plot the virtual photon structure function $g_1^\gamma(x, Q^2, P^2)$ in the NLO for $N_f = 3$, $Q^2 = 30\,\mathrm{GeV}^2$ and $P^2 = 1\,\mathrm{GeV}^2$ and the QCD scale parameter $\Lambda = 0.2\,\mathrm{GeV}$. The vertical axis corresponds to

$$g_1^\gamma(x, Q^2, P^2)/\frac{3\alpha}{\pi}N_f\langle e^4\rangle \ln\frac{Q^2}{P^2}. \tag{6.2}$$

Also shown are the LO result, the box (tree) diagram contribution,

$$g_1^{\gamma(\mathrm{box})}(x, Q^2, P^2) = (2x-1)\frac{3\alpha}{\pi}N_f\langle e^4\rangle \ln\frac{Q^2}{P^2}, \tag{6.3}$$

and the box diagram contribution including the non-leading (NL) correction with mass being ignored,

$$g_1^{\gamma(\mathrm{box(NL)})}(x, Q^2, P^2) = \frac{3\alpha}{\pi}N_f\langle e^4\rangle$$

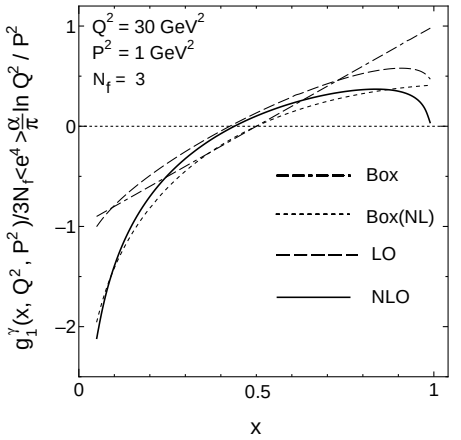


**Fig. 6.** Polarized virtual photon structure function $g_1^\gamma(x, Q^2, P^2)$ up to NLO in units of $(3N_f\alpha\langle e^4\rangle/\pi)\ln(Q^2/P^2)$ for $Q^2 = 30\,\mathrm{GeV}^2$, and $P^2 = 1\,\mathrm{GeV}^2$ and the QCD scale parameter $\Lambda = 0.2\,\mathrm{GeV}$ with $N_f = 3$ (solid line). We also plot the LO result (long-dashed line), the box (tree) diagram (2dash-dotted line) and the box including non-leading contribution, box (NL) (short-dashed line)

$$\times\left[(2x-1)\ln\frac{Q^2}{P^2} - 2(2x-1)(\ln x + 1)\right]. \tag{6.4}$$

In our previous paper [23], there was an error in the program for the numerical evaluation of the NLO $g_1^\gamma(x, Q^2, P^2)$. The corrected graph (NLO curve) here is different from the corresponding one in Fig. 2 of [23]. The new NLO curve appears lower than the previous one for $x < 0.7$ and rather enhanced above $x = 0.7$. We observe that the corrected NLO curve remains below the LO one, and that the NLO QCD corrections are significant at large $x$ as well as at low $x$.

For the case of the real photon target, $P^2 = 0$, the structure function can be decomposed as

$$g_1^\gamma(x, Q^2) = g_1^\gamma(x, Q^2)|_{\mathrm{pert.}} + g_1^\gamma(x, Q^2)|_{\mathrm{non-pert.}}. \tag{6.5}$$

The first term, the point-like piece, can be calculated by a perturbative method. Actually, it can be obtained by setting $P^2 = \Lambda^2$ in the expressions of parton distributions in (2.2) or (2.3). The second term can only be computed by some non-perturbative methods. In Fig. 7, we plot the point-like piece of the real photon $g_1^\gamma(x, Q^2)$ in the NLO, together with the LO result and the box (tree) diagram contribution. The NLO curve, which is calculated by the corrected computer program, is different from the previous one in Fig. 6 in [23]. The new NLO curve appears to be lower than the previous one for $x < 0.6$ and enhanced above $x = 0.6$. Also it remains below the LO curve. The NLO result is qualitatively consistent with the analysis by Stratmann and Vogelsang [18]. In the unpolarized case, the moment of $F_2^\gamma$ has a singularity at $n = 2$ which leads to the negative structure function at low $x$. Thus we need some regularization prescription to recover a positive structure function as discussed in [54–56]. Note that we do not have such a complication at $n = 1$ for the polarized case.

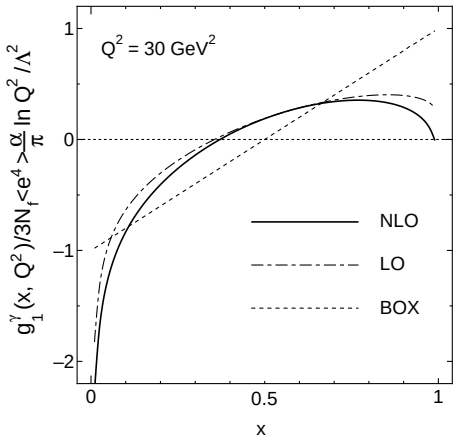


**Fig. 7.** Point-like piece of the real photon structure function $g_1^\gamma(x,Q^2)$ in NLO in units of $(3N_f\alpha\langle e^4\rangle/\pi)\ln(Q^2/\Lambda^2)$ for $Q^2 = 30\,\mathrm{GeV}^2$ with $\Lambda = 0.2\,\mathrm{GeV}$, $N_f = 3$ (solid line). Also plotted are the LO result (long-dashed line) and the box (tree) diagram contribution (short-dashed line)

Finally, in our numerical analysis, we took $P^2 = 1\,\mathrm{GeV}^2$, which may not be necessarily large enough for the non-perturbative effects to be dying away. For our *normalized* parton distributions, however, the larger values of $P^2$ would not give any sizable change in shape and magnitude.

## 7 Conclusion

In the present paper, we have studied in detail the spin-dependent parton distributions inside the virtual photon, which can be predicted entirely up to NLO in perturbative QCD. The virtual photon target provides a good testing ground for examining the factorization-scheme dependence of the quark and gluon distributions. We have investigated the polarized parton distributions in several different factorization schemes. We derived the explicit transformation rules from one scheme to another for the coefficient functions, the finite photon matrix elements and the two-loop anomalous dimensions or parton splitting functions.

In particular, we studied the QCD and QED axial anomaly effects on the first moments of the quark distributions to see the interplay between the axial anomalies and factorization schemes. We find that, in the CI-like schemes, the first moments of the polarized quark distributions, both flavor singlet and non-singlet, vanish in NLO while the standard $\overline{\mathrm{MS}}$ scheme gives a non-zero value. Also we find that the large-$x$ behaviors of the polarized quark distributons dramatically vary from one factorization scheme to another. Indeed, for $x \to 1$, the quark distributions positively diverge or negatively diverge or remain finite, depending on the factorization schemes. The numerical analyses performed for the parton distributions reconfirm the above observations. From the viewpoint of "perturbative stabilities" the OS scheme gives more appropriate behaviors for the quark distributions than the others. The gluon distribution turns out to be the same up to NLO among the six factorization schemes examined. Furthermore, its first moment is found to be factorization-scheme independent up to NLO.

The same analysis of the factorization-scheme dependence of the unpolarized parton distributions of the virtual photon can be carried out and will be discussed elsewhere.

*Acknowledgements.* We thank J. Blümlein, S.J. Brodsky, J. Kodaira, M. Stratmann, O.V. Teryaev and W.L. van Neerven for valuable discussions. One of the authors (K.S.) would like to thank J. Blümlein and T. Riemann for the hospitality extended to him at the 5th Zeuthen Workshop "Loops and Legs 2000". Some of the results in this paper have been reported at the workshop. We also thank E. Reya and C. Sieg for the communication regarding the numerical evaluation of the structure function. This work is partially supported by the Monbusho Grant-in-Aid for Scientific Research NO.(C)(2)-12640266.

## Appendix

## A NLO expressions for polarized parton distributions in the virtual photon

We give the explicit expressions of $\Delta q_{\mathrm{S}}^\gamma$, $\Delta G^\gamma$, and $\Delta q_{\mathrm{NS}}^\gamma$ up to NLO. They are written in terms of one- (two-) loop anomalous dimensions $\Delta\gamma_{ij}^{0,n}$ ($\Delta\gamma_{ij}^{(1),n}$) ($i,j = \psi, G$), $\Delta\gamma_{\mathrm{NS}}^{0,n}$ ($\gamma_{\mathrm{NS}}^{(1),n}$), $\Delta K_l^{0,n}$ ($\Delta K_l^{(1),n}$) ($l = \psi, G, \mathrm{NS}$), and the one-loop photon matrix elements of the hadronic operators, $\Delta A_l^n$. The expressions of one-loop and $\overline{\mathrm{MS}}$ scheme two-loop anomalous dimensions are found, for example, in the appendix of [23].

### A.1 Singlet quark distribution

$$
\begin{aligned}
&\Delta q_{\mathrm{S}}^\gamma(n,Q^2,P^2)/\frac{\alpha}{8\pi\beta_0} \\
&= \frac{4\pi}{\alpha_{\mathrm{s}}(Q^2)}\hat{L}_{\mathrm{S}}^{+n}\left\{1-\left[\frac{\alpha_{\mathrm{s}}(Q^2)}{\alpha_{\mathrm{s}}(P^2)}\right]^{\lambda_+^n/2\beta_0+1}\right\} \\
&+\frac{4\pi}{\alpha_{\mathrm{s}}(Q^2)}\hat{L}_{\mathrm{S}}^{-n}\left\{1-\left[\frac{\alpha_{\mathrm{s}}(Q^2)}{\alpha_{\mathrm{s}}(P^2)}\right]^{\lambda_-^n/2\beta_0+1}\right\} \\
&+\hat{A}_{\mathrm{S}}^{+n}\left\{1-\left[\frac{\alpha_{\mathrm{s}}(Q^2)}{\alpha_{\mathrm{s}}(P^2)}\right]^{\lambda_+^n/2\beta_0}\right\} \\
&+\hat{A}_{\mathrm{S}}^{-n}\left\{1-\left[\frac{\alpha_{\mathrm{s}}(Q^2)}{\alpha_{\mathrm{s}}(P^2)}\right]^{\lambda_-^n/2\beta_0}\right\} \\
&+\hat{B}_{\mathrm{S}}^{+n}\left\{1-\left[\frac{\alpha_{\mathrm{s}}(Q^2)}{\alpha_{\mathrm{s}}(P^2)}\right]^{\lambda_+^n/2\beta_0+1}\right\} \\
&+\hat{B}_{\mathrm{S}}^{-n}\left\{1-\left[\frac{\alpha_{\mathrm{s}}(Q^2)}{\alpha_{\mathrm{s}}(P^2)}\right]^{\lambda_-^n/2\beta_0+1}\right\} \\
&+\hat{C}_{\mathrm{S}}^n, \qquad \text{(A.1)}
\end{aligned}
$$

where

$$\hat{L}_{\rm S}^{+n} = \Delta K_\psi^{0,n} \cdot \frac{\Delta\gamma_{\psi\psi}^{0,n} - \lambda_-^n}{\lambda_+^n - \lambda_-^n} \cdot \frac{1}{1+\lambda_+^n/2\beta_0}, \quad \text{(A.2)}$$

$$\hat{L}_{\rm S}^{-n} = \Delta K_\psi^{0,n} \cdot \frac{\Delta\gamma_{\psi\psi}^{0,n} - \lambda_+^n}{\lambda_-^n - \lambda_+^n} \cdot \frac{1}{1+\lambda_-^n/2\beta_0}, \quad \text{(A.3)}$$

with

$$\lambda_\pm^n = \frac{1}{2}\{\Delta\gamma_{\psi\psi}^{0,n} + \Delta\gamma_{GG}^{0,n} \pm [(\Delta\gamma_{\psi\psi}^{0,n} - \Delta\gamma_{GG}^{0,n})^2 + 4\Delta\gamma_{\psi G}^{0,n}\Delta\gamma_{G\psi}^{0,n}]^{1/2}\}, \quad \text{(A.4)}$$

$$\beta_0 = 11 - 2N_f/3, \quad \beta_1 = 102 - 38N_f/3, \quad \text{(A.5)}$$

and

$$\begin{aligned}\hat{A}_{\rm S}^{+n} = {} & \frac{1}{\lambda_+^n(\lambda_+^n-\lambda_-^n)(2\beta_0+\lambda_-^n-\lambda_+^n)} \\ & \times \Big[\Delta K_\psi^{0,n}\Big\{(\Delta\gamma_{\psi\psi}^{0,n} - 2\beta_0 - \lambda_-^n)\Delta\gamma_{\psi\psi}^{(1),n} \\ & + \Delta\gamma_{G\psi}^{0,n}\Delta\gamma_{\psi G}^{(1),n}\Big\}(\Delta\gamma_{\psi\psi}^{0,n} - \lambda_-^n) \\ & + \Delta K_\psi^{0,n}\Big\{(\Delta\gamma_{\psi\psi}^{0,n} - 2\beta_0 - \lambda_-^n)\Delta\gamma_{G\psi}^{(1),n} \\ & + \Delta\gamma_{G\psi}^{0,n}\Delta\gamma_{GG}^{(1),n}\Big\}\Delta\gamma_{\psi G}^{0,n} \\ & + 2\beta_0(2\beta_0 + \lambda_-^n - \lambda_+^n) \\ & \times \Big\{\Delta K_\psi^{(1),n}(\Delta\gamma_{\psi\psi}^{0,n} - \lambda_-^n) + \Delta K_G^{(1),n}\Delta\gamma_{\psi G}^{0,n}\Big\} \\ & - 2\beta_0(2\beta_0 + \lambda_-^n - \lambda_+^n)\lambda_+^n\Delta A_\psi^n(\Delta\gamma_{\psi\psi}^{0,n} - \lambda_-^n) \\ & - \frac{\beta_1}{\beta_0}\Delta K_\psi^{0,n}(2\beta_0 + \lambda_-^n - \lambda_+^n)(2\beta_0 - \lambda_+^n) \\ & \times (\Delta\gamma_{\psi\psi}^{0,n} - \lambda_-^n)\Big], \end{aligned} \quad \text{(A.6)}$$

$$\begin{aligned}\hat{A}_{\rm S}^{-n} = {} & \frac{1}{\lambda_-^n(\lambda_-^n-\lambda_+^n)(2\beta_0+\lambda_+^n-\lambda_-^n)} \\ & \times \Big[\Delta K_\psi^{0,n}\Big\{(\Delta\gamma_{\psi\psi}^{0,n} - 2\beta_0 - \lambda_+^n)\Delta\gamma_{\psi\psi}^{(1),n} \\ & + \Delta\gamma_{G\psi}^{0,n}\Delta\gamma_{\psi G}^{(1),n}\Big\}(\Delta\gamma_{\psi\psi}^{0,n} - \lambda_+^n) \\ & + \Delta K_\psi^{0,n}\Big\{(\Delta\gamma_{\psi\psi}^{0,n} - 2\beta_0 - \lambda_+^n)\Delta\gamma_{G\psi}^{(1),n} \\ & + \Delta\gamma_{G\psi}^{0,n}\Delta\gamma_{GG}^{(1),n}\Big\}\Delta\gamma_{\psi G}^{0,n} \\ & + 2\beta_0(2\beta_0 + \lambda_+^n - \lambda_-^n) \\ & \times \Big\{\Delta K_\psi^{(1),n}(\Delta\gamma_{\psi\psi}^{0,n} - \lambda_+^n) + \Delta K_G^{(1),n}\Delta\gamma_{\psi G}^{0,n}\Big\} \\ & - 2\beta_0(2\beta_0 + \lambda_+^n - \lambda_-^n)\lambda_-^n\Delta A_\psi^n(\Delta\gamma_{\psi\psi}^{0,n} - \lambda_+^n) \\ & - \frac{\beta_1}{\beta_0}\Delta K_\psi^{0,n}(2\beta_0 + \lambda_+^n - \lambda_-^n)(2\beta_0 - \lambda_-^n) \\ & \times (\Delta\gamma_{\psi\psi}^{0,n} - \lambda_+^n)\Big], \end{aligned} \quad \text{(A.7)}$$

$$\begin{aligned}\hat{B}_{\rm S}^{+n} = {} & \Delta K_\psi^{0,n} \cdot \frac{1}{(2\beta_0+\lambda_+^n)(\lambda_+^n-\lambda_-^n)(2\beta_0+\lambda_+^n-\lambda_-^n)} \\ & \times \Big[\Big\{(\Delta\gamma_{\psi\psi}^{0,n} - \lambda_-^n)\Delta\gamma_{\psi\psi}^{(1),n} + \Delta\gamma_{G\psi}^{0,n}\Delta\gamma_{\psi G}^{(1),n}\Big\} \\ & \times (2\beta_0 + \Delta\gamma_{\psi\psi}^{0,n} - \lambda_-^n) \\ & + \Big\{(\Delta\gamma_{\psi\psi}^{0,n} - \lambda_-^n)\Delta\gamma_{G\psi}^{(1),n} + \Delta\gamma_{G\psi}^{0,n}\Delta\gamma_{GG}^{(1),n}\Big\}\Delta\gamma_{\psi G}^{0,n} \\ & - \frac{\beta_1}{\beta_0}(2\beta_0 + \lambda_+^n - \lambda_-^n)\lambda_+^n(\Delta\gamma_{\psi\psi}^{0,n} - \lambda_-^n)\Big], \end{aligned} \quad \text{(A.8)}$$

$$\begin{aligned}\hat{B}_{\rm S}^{-n} = {} & \Delta K_\psi^{0,n} \cdot \frac{1}{(2\beta_0+\lambda_-^n)(\lambda_-^n-\lambda_+^n)(2\beta_0+\lambda_-^n-\lambda_+^n)} \\ & \times \Big[\Big\{(\Delta\gamma_{\psi\psi}^{0,n} - \lambda_+^n)\Delta\gamma_{\psi\psi}^{(1),n} + \Delta\gamma_{G\psi}^{0,n}\Delta\gamma_{\psi G}^{(1),n}\Big\} \\ & \times (2\beta_0 + \Delta\gamma_{\psi\psi}^{0,n} - \lambda_+^n) \\ & + \Big\{(\Delta\gamma_{\psi\psi}^{0,n} - \lambda_+^n)\Delta\gamma_{G\psi}^{(1),n} + \Delta\gamma_{G\psi}^{0,n}\Delta\gamma_{GG}^{(1),n}\Big\}\Delta\gamma_{\psi G}^{0,n} \\ & - \frac{\beta_1}{\beta_0}(2\beta_0 + \lambda_-^n - \lambda_+^n)\lambda_-^n(\Delta\gamma_{\psi\psi}^{0,n} - \lambda_+^n)\Big], \\ \hat{C}_{\rm S}^n = {} & 2\beta_0\Delta A_\psi^n. \end{aligned} \quad \text{(A.9)}$$

## A.2 Gluon distribution

$$\begin{aligned}\Delta G^\gamma(n,Q^2,P^2)/\frac{\alpha}{8\pi\beta_0} = {} & \frac{4\pi}{\alpha_{\rm s}(Q^2)}\hat{L}_G^{+n}\left\{1 - \left[\frac{\alpha_{\rm s}(Q^2)}{\alpha_{\rm s}(P^2)}\right]^{\lambda_+^n/2\beta_0+1}\right\} \\ & + \frac{4\pi}{\alpha_{\rm s}(Q^2)}\hat{L}_G^{-n}\left\{1 - \left[\frac{\alpha_{\rm s}(Q^2)}{\alpha_{\rm s}(P^2)}\right]^{\lambda_-^n/2\beta_0+1}\right\} \\ & + \hat{A}_G^{+n}\left\{1 - \left[\frac{\alpha_{\rm s}(Q^2)}{\alpha_{\rm s}(P^2)}\right]^{\lambda_+^n/2\beta_0}\right\} \\ & + \hat{A}_G^{-n}\left\{1 - \left[\frac{\alpha_{\rm s}(Q^2)}{\alpha_{\rm s}(P^2)}\right]^{\lambda_-^n/2\beta_0}\right\} \\ & + \hat{B}_G^{+n}\left\{1 - \left[\frac{\alpha_{\rm s}(Q^2)}{\alpha_{\rm s}(P^2)}\right]^{\lambda_+^n/2\beta_0+1}\right\} \\ & + \hat{B}_G^{-n}\left\{1 - \left[\frac{\alpha_{\rm s}(Q^2)}{\alpha_{\rm s}(P^2)}\right]^{\lambda_-^n/2\beta_0+1}\right\}, \end{aligned} \quad \text{(A.10)}$$

where

$$\hat{L}_G^{+n} = \frac{\Delta K_\psi^{0,n}\Delta\gamma_{G\psi}^{0,n}}{\lambda_+^n - \lambda_-^n} \cdot \frac{1}{1+\lambda_+^n/2\beta_0}, \quad \text{(A.11)}$$

$$\hat{L}_G^{-n} = \frac{\Delta K_\psi^{0,n}\Delta\gamma_{G\psi}^{0,n}}{\lambda_-^n - \lambda_+^n} \cdot \frac{1}{1+\lambda_-^n/2\beta_0}, \quad \text{(A.12)}$$

and

$$\begin{aligned}\hat{A}_G^{+n} = {} & \frac{1}{\lambda_+^n(\lambda_+^n-\lambda_-^n)(2\beta_0+\lambda_-^n-\lambda_+^n)} \\ & \times \Big[\Delta K_\psi^{0,n}\Big\{(\Delta\gamma_{\psi\psi}^{0,n} - 2\beta_0 - \lambda_-^n)\Delta\gamma_{\psi\psi}^{(1),n}\end{aligned}$$

$$
\begin{aligned}
&+ \Delta\gamma_{G\psi}^{0,n}\Delta\gamma_{\psi G}^{(1),n}\Big\}\,\Delta\gamma_{G\psi}^{0,n} \\
&+ \Delta K_{\psi}^{0,n}\Big\{(\Delta\gamma_{\psi\psi}^{0,n}-2\beta_0-\lambda_-^n)\Delta\gamma_{G\psi}^{(1),n} \\
&+ \Delta\gamma_{G\psi}^{0,n}\Delta\gamma_{GG}^{(1),n}\Big\}(\Delta\gamma_{GG}^{0,n}-\lambda_-^n) \\
&+ 2\beta_0(2\beta_0+\lambda_-^n-\lambda_+^n) \\
&\times\Big\{\Delta K_{\psi}^{(1),n}\Delta\gamma_{G\psi}^{0,n}+\Delta K_{G}^{(1),n}(\Delta\gamma_{GG}^{0,n}-\lambda_-^n)\Big\} \\
&- 2\beta_0(2\beta_0+\lambda_-^n-\lambda_+^n)\lambda_+^n\Delta A_{\psi}^n\Delta\gamma_{G\psi}^{0,n} \qquad \text{(A.13)} \\
&- \frac{\beta_1}{\beta_0}\Delta K_{\psi}^{0,n}(2\beta_0+\lambda_-^n-\lambda_+^n)(2\beta_0-\lambda_+^n)\Delta\gamma_{G\psi}^{0,n}\Big],
\end{aligned}
$$

$$
\begin{aligned}
\hat{A}_G^{-n} &= \frac{1}{\lambda_-^n(\lambda_-^n-\lambda_+^n)(2\beta_0+\lambda_+^n-\lambda_-^n)} \\
&\times\Big[\Delta K_{\psi}^{0,n}\Big\{(\Delta\gamma_{\psi\psi}^{0,n}-2\beta_0-\lambda_+^n)\Delta\gamma_{\psi\psi}^{(1),n} \\
&+ \Delta\gamma_{G\psi}^{0,n}\Delta\gamma_{\psi G}^{(1),n}\Big\}\Delta\gamma_{G\psi}^{0,n} \\
&+ \Delta K_{\psi}^{0,n}\Big\{(\Delta\gamma_{\psi\psi}^{0,n}-2\beta_0-\lambda_+^n)\Delta\gamma_{G\psi}^{(1),n} \\
&+ \Delta\gamma_{G\psi}^{0,n}\Delta\gamma_{GG}^{(1),n}\Big\}(\Delta\gamma_{GG}^{0,n}-\lambda_+^n) \\
&+ 2\beta_0(2\beta_0+\lambda_+^n-\lambda_-^n) \\
&\times\Big\{\Delta K_{\psi}^{(1),n}\Delta\gamma_{G\psi}^{0,n}+\Delta K_{G}^{(1),n}(\Delta\gamma_{GG}^{0,n}-\lambda_+^n)\Big\} \\
&- 2\beta_0(2\beta_0+\lambda_+^n-\lambda_-^n)\lambda_-^n\Delta A_{\psi}^n\Delta\gamma_{G\psi}^{0,n} \qquad \text{(A.14)} \\
&- \frac{\beta_1}{\beta_0}\Delta K_{\psi}^{0,n}(2\beta_0+\lambda_+^n-\lambda_-^n)(2\beta_0-\lambda_-^n)\Delta\gamma_{G\psi}^{0,n}\Big],
\end{aligned}
$$

$$
\begin{aligned}
\hat{B}_G^{+n} &= \Delta K_{\psi}^{0,n}\cdot\frac{1}{(2\beta_0+\lambda_+^n)(\lambda_+^n-\lambda_-^n)(2\beta_0+\lambda_+^n-\lambda_-^n)} \\
&\times\Big[\Big\{(\Delta\gamma_{\psi\psi}^{0,n}-\lambda_-^n)\Delta\gamma_{G\psi}^{(1),n}+\Delta\gamma_{G\psi}^{0,n}\Delta\gamma_{GG}^{(1),n}\Big\} \\
&\times(2\beta_0+\Delta\gamma_{GG}^{0,n}-\lambda_-^n) \\
&+\Big\{(\Delta\gamma_{\psi\psi}^{0,n}-\lambda_-^n)\Delta\gamma_{\psi\psi}^{(1),n}+\Delta\gamma_{G\psi}^{0,n}\Delta\gamma_{\psi G}^{(1),n}\Big\}\Delta\gamma_{G\psi}^{0,n} \\
&-\frac{\beta_1}{\beta_0}(2\beta_0+\lambda_+^n-\lambda_-^n)\lambda_+^n\Delta\gamma_{G\psi}^{0,n}\Big], \qquad \text{(A.15)}
\end{aligned}
$$

$$
\begin{aligned}
\hat{B}_G^{-n} &= \Delta K_{\psi}^{0,n}\cdot\frac{1}{(2\beta_0+\lambda_-^n)(\lambda_-^n-\lambda_+^n)(2\beta_0+\lambda_-^n-\lambda_+^n)} \\
&\times\Big[\Big\{(\Delta\gamma_{\psi\psi}^{0,n}-\lambda_+^n)\Delta\gamma_{G\psi}^{(1),n}+\Delta\gamma_{G\psi}^{0,n}\Delta\gamma_{GG}^{(1),n}\Big\} \\
&\times(2\beta_0+\Delta\gamma_{GG}^{0,n}-\lambda_+^n) \\
&+\Big\{(\Delta\gamma_{\psi\psi}^{0,n}-\lambda_+^n)\Delta\gamma_{\psi\psi}^{(1),n}+\Delta\gamma_{G\psi}^{0,n}\Delta\gamma_{\psi G}^{(1),n}\Big\}\Delta\gamma_{G\psi}^{0,n} \\
&-\frac{\beta_1}{\beta_0}(2\beta_0+\lambda_-^n-\lambda_+^n)\lambda_-^n\Delta\gamma_{G\psi}^{0,n}\Big]. \qquad \text{(A.16)}
\end{aligned}
$$

### A.3 Non-singlet quark

$$
\begin{aligned}
&\Delta q_{\rm NS}^{\gamma}(n,Q^2,P^2)/\frac{\alpha}{8\pi\beta_0} \\
&= \frac{4\pi}{\alpha_{\rm s}(Q^2)}\hat{L}_{\rm NS}^n\left\{1-\left[\frac{\alpha_{\rm s}(Q^2)}{\alpha_{\rm s}(P^2)}\right]^{\lambda_{\rm NS}^n/2\beta_0+1}\right\} \\
&+\hat{A}_{\rm NS}^n\left\{1-\left[\frac{\alpha_{\rm s}(Q^2)}{\alpha_{\rm s}(P^2)}\right]^{\lambda_{\rm NS}^n/2\beta_0}\right\} \\
&+\hat{B}_{\rm NS}^n\left\{1-\left[\frac{\alpha_{\rm s}(Q^2)}{\alpha_{\rm s}(P^2)}\right]^{\lambda_{\rm NS}^n/2\beta_0+1}\right\} \\
&+\hat{C}_{\rm NS}^n, \qquad \text{(A.17)}
\end{aligned}
$$

where

$$
\hat{L}_{\rm NS}^n = \Delta K_{\rm NS}^{0,n}\cdot\frac{1}{1+\lambda_{\rm NS}^n/2\beta_0}, \qquad \text{(A.18)}
$$

$$
\begin{aligned}
\hat{A}_{\rm NS}^n &= \frac{1}{\lambda_{\rm NS}^n}\Big\{-\Delta K_{\rm NS}^{0,n}\Delta\gamma_{\rm NS}^{(1),n}+2\beta_0\Delta K_{\rm NS}^{(1),n} \\
&- 2\beta_0\lambda_{\rm NS}^n\Delta A_{\rm NS}^n-\frac{\beta_1}{\beta_0}\Delta K_{\rm NS}^{0,n}(2\beta_0-\lambda_{\rm NS}^n)\Big\}, \qquad \text{(A.19)}
\end{aligned}
$$

$$
\hat{B}_{\rm NS}^n = \Delta K_{\rm NS}^{0,n}\frac{1}{2\beta_0+\lambda_{\rm NS}^n}\left(\Delta\gamma_{\rm NS}^{(1),n}-\frac{\beta_1}{\beta_0}\lambda_{\rm NS}^n\right), \qquad \text{(A.20)}
$$

$$
\hat{C}_{\rm NS}^n = 2\beta_0\Delta A_{\rm NS}^n, \qquad \text{(A.21)}
$$

with

$$
\lambda_{\rm NS}^n = \Delta\gamma_{\rm NS}^{0,n}. \qquad \text{(A.22)}
$$

## B The first moments

### B.1 One-loop order

$$
\Delta\gamma_{\rm NS}^{0,n=1} = \Delta\gamma_{\psi\psi}^{0,n=1} = 0, \qquad \text{(B.1)}
$$

$$
\Delta\gamma_{\psi G}^{0,n=1} = 0, \quad \Delta\gamma_{G\psi}^{0,n=1} = -6C_F, \qquad \text{(B.2)}
$$

$$
\Delta\gamma_{GG}^{0,n=1} = -\frac{22}{3}C_A+\frac{8}{3}T_f = -2\beta_0, \qquad \text{(B.3)}
$$

$$
\lambda_+^{n=1} = 0, \quad \lambda_-^{n=1} = -2\beta_0, \qquad \text{(B.4)}
$$

$$
\Delta K_{\rm NS}^{0,n=1} = \Delta K_{\psi}^{0,n=1} = 0, \qquad \text{(B.5)}
$$

where

$$
C_A = 3, \quad C_F = \frac{4}{3}, \quad T_f = \frac{N_f}{2}, \qquad \text{(B.6)}
$$

with $N_f$ being the number of flavors.

### B.2 $\overline{\rm MS}$ scheme

$$
\Delta\gamma_{{\rm NS},\overline{\rm MS}}^{(1),n=1} = 0, \qquad \text{(B.7)}
$$

$$
\Delta\gamma_{\psi\psi,\overline{\rm MS}}^{(1),n=1} = 24C_FT_f, \qquad \text{(B.8)}
$$

$$
\Delta\gamma_{\psi G,\overline{\rm MS}}^{(1),n=1} = 0, \qquad \text{(B.9)}
$$

$$
\Delta\gamma_{G\psi,\overline{\rm MS}}^{(1),n=1} = 18C_F^2-\frac{142}{3}C_AC_F+\frac{8}{3}C_FT_f, \qquad \text{(B.10)}
$$

$$\Delta\gamma_{GG,\overline{\rm MS}}^{(1),n=1} = 8C_F T_f + \frac{40}{3}C_A T_f - \frac{68}{3}C_A^2 = -2\beta_1, \tag{B.11}$$

$$\Delta K_{\psi,\overline{\rm MS}}^{(1),n=1} = \Delta K_{G,\overline{\rm MS}}^{(1),n=1} = \Delta K_{\rm NS,\overline{\rm MS}}^{(1),n=1} = 0, \tag{B.12}$$

$$\Delta A_{\psi,\overline{\rm MS}}^{n=1} = -12\langle e^2\rangle N_f, \tag{B.13}$$

$$\Delta A_{G,\overline{\rm MS}}^{n=1} = 0, \tag{B.14}$$

$$\Delta A_{\rm NS,\overline{\rm MS}}^{n=1} = -12(\langle e^4\rangle - \langle e^2\rangle^2)N_f, \tag{B.15}$$

$$\Delta B_{\psi,\overline{\rm MS}}^{n=1} = \Delta B_{\rm NS,\overline{\rm MS}}^{n=1} = -3C_F, \tag{B.16}$$

$$\Delta B_{G,\overline{\rm MS}}^{n=1} = \frac{N_f}{2}\Delta B_{\gamma,\overline{\rm MS}}^{n=1} = 0. \tag{B.17}$$

### B.3 CI-like schemes (CI, AB, OS, AR)

$$\Delta\gamma_{{\rm NS},a}^{(1),n=1} = 0, \tag{B.18}$$

$$\Delta\gamma_{\psi\psi,a}^{(1),n=1} = 0, \tag{B.19}$$

$$\Delta\gamma_{\psi G,a}^{(1),n=1} = \Delta\gamma_{\psi G,\overline{\rm MS}}^{(1),n=1} = 0, \tag{B.20}$$

$$\begin{aligned}\Delta\gamma_{G\psi,a}^{(1),n=1} &= \Delta\gamma_{G\psi,\overline{\rm MS}}^{(1),n=1} \\ &= 18C_F^2 - \frac{142}{3}C_A C_F + \frac{8}{3}C_F T_f,\end{aligned} \tag{B.21}$$

$$\begin{aligned}\Delta\gamma_{GG,a}^{(1),n=1} &= 32C_F T_f + \frac{40}{3}C_A T_f - \frac{68}{3}C_A^2 \\ &= -2\beta_1 + 12N_f C_F,\end{aligned} \tag{B.22}$$

$$\Delta K_{\psi,a}^{(1),n=1} = \Delta K_{{\rm NS},a}^{(1),n=1} = 0, \tag{B.23}$$

$$\Delta K_{G,a}^{(1),n=1} = -72\langle e^2\rangle N_f C_F, \tag{B.24}$$

$$\Delta A_{\psi,a}^{n=1} = \Delta A_{G,a}^{n=1} = \Delta A_{{\rm NS},a}^{n=1} = 0, \tag{B.25}$$

$$\Delta B_{\psi,a}^{n=1} = \Delta B_{{\rm NS},a}^{n=1} = -3C_F, \tag{B.26}$$

$$\Delta B_{G,a}^{n=1} = \frac{N_f}{2}\Delta B_{\gamma,a}^{n=1} = -2N_f. \tag{B.27}$$

## C Derivation of (4.20) and (4.21)

We observe that, in the $\overline{\rm MS}$ scheme, we have $\Delta\boldsymbol{K}^{0,n=1} = \Delta\boldsymbol{K}^{(1),n=1} = 0$, where $\Delta\boldsymbol{K}^n = (\Delta K_\psi^n, \Delta K_G^n, \Delta K_{\rm NS}^n)$. (Note that $\Delta K_{G,{\rm CI-like}}^{(1),n=1} \neq 0$; see (B.24).) Then, up to NLO, the parton distributions $\Delta\boldsymbol{q}^\gamma(n=1)|_{\overline{\rm MS}} = (\Delta q_{\rm S}^\gamma, \Delta G^\gamma, \Delta q_{\rm NS}^\gamma)|_{\overline{\rm MS}}$ satisfy a homogeneous differential equation instead of an inhomogeneous one:

$$\begin{aligned}&\frac{{\rm d}\Delta\boldsymbol{q}^\gamma(n=1,Q^2,P^2)|_{\overline{\rm MS}}}{{\rm d}\ln Q^2} \\ &\quad = \Delta\boldsymbol{q}^\gamma(n=1,Q^2,P^2)|_{\overline{\rm MS}}\Delta P(n=1,Q^2)|_{\overline{\rm MS}},\end{aligned} \tag{C.1}$$

where the $3\times 3$ splitting function matrix $\Delta P$ is the hadronic part of $\Delta\widetilde{P}$ given in (3.1). Expanding $\Delta P(n=1,Q^2)|_{\overline{\rm MS}}$ as

$$\Delta P(n=1,Q^2)|_{\overline{\rm MS}} = \frac{\alpha_{\rm s}(Q^2)}{2\pi}\Delta P_{n=1}^{(0)} + \left[\frac{\alpha_{\rm s}(Q^2)}{2\pi}\right]^2 \Delta P_{n=1}^{(1)}|_{\overline{\rm MS}} + \cdots, \tag{C.2}$$

and introducing $t$ instead of $Q^2$ as the evolution variable,

$$t \equiv \frac{2}{\beta_0}\ln\frac{\alpha_{\rm s}(P^2)}{\alpha_{\rm s}(Q^2)}, \tag{C.3}$$

we find that (C.1) is rewritten as

$$\begin{aligned}\frac{{\rm d}\Delta\boldsymbol{q}_{n=1}^\gamma(t)|_{\overline{\rm MS}}}{{\rm d}t} &= \Delta\boldsymbol{q}_{n=1}^\gamma(t)|_{\overline{\rm MS}}\Big\{\Delta P_{n=1}^{(0)} \\ &+ \frac{\alpha_{\rm s}(t)}{2\pi}\left[\Delta P_{n=1}^{(1)}|_{\overline{\rm MS}} - \frac{\beta_1}{2\beta_0}\Delta P_{n=1}^{(0)}\right] + \mathcal{O}(\alpha_{\rm s}^2)\Big\}.\end{aligned} \tag{C.4}$$

We look for a solution in the following form:

$$\Delta\boldsymbol{q}_{n=1}^\gamma(t)|_{\overline{\rm MS}} = \Delta\boldsymbol{q}_{n=1}^{\gamma(0)}(t) + \Delta\boldsymbol{q}_{n=1}^{\gamma(1)}(t)|_{\overline{\rm MS}}, \tag{C.5}$$

with the initial condition (see (2.5)),

$$\Delta\boldsymbol{q}_{n=1}^{\gamma(0)}(0) = 0, \tag{C.6}$$

$$\begin{aligned}\Delta\boldsymbol{q}_{n=1}^{\gamma(1)}(0)|_{\overline{\rm MS}} &= \frac{\alpha}{4\pi}\Delta\boldsymbol{A}_{n=1}|_{\overline{\rm MS}} \\ &= -\frac{3\alpha}{\pi}N_f(\langle e^2\rangle, 0, \langle e^4\rangle - \langle e^2\rangle^2).\end{aligned} \tag{C.7}$$

In the LO, we easily find that $\Delta\boldsymbol{q}_{n=1}^{\gamma(0)}(t) = 0$ due to the initial condition (C.6).

The evolution equation in the NLO is written as

$$\begin{aligned}\frac{{\rm d}\Delta\boldsymbol{q}_{n=1}^{\gamma(1)}(t)|_{\overline{\rm MS}}}{{\rm d}t} &= \Delta\boldsymbol{q}_{n=1}^{\gamma(1)}(t)|_{\overline{\rm MS}}\Big\{\Delta P_{n=1}^{(0)} \\ &+ \frac{\alpha_{\rm s}(t)}{2\pi}\left[\Delta P_{n=1}^{(1)}|_{\overline{\rm MS}} - \frac{\beta_1}{2\beta_0}\Delta P_{n=1}^{(0)}\right]\Big\},\end{aligned} \tag{C.8}$$

and we obtain for the solution

$$\Delta\boldsymbol{q}_{n=1}^{\gamma(1)}(t)|_{\overline{\rm MS}} = \Delta\boldsymbol{q}_{n=1}^{\gamma(1)}(0)|_{\overline{\rm MS}}\exp(M), \tag{C.9}$$

where

$$\begin{aligned}M &= \Delta P_{n=1}^{(0)}t + \frac{1}{\beta_0}\left[\frac{\alpha_{\rm s}(0)}{\pi} - \frac{\alpha_{\rm s}(t)}{\pi}\right] \\ &\times \left[\Delta P_{n=1}^{(1)}|_{\overline{\rm MS}} - \frac{\beta_1}{2\beta_0}\Delta P_{n=1}^{(0)}\right].\end{aligned} \tag{C.10}$$

Since

$$\Delta P_{n=1}^{(0)} = -\frac{1}{4}\Delta\hat{\gamma}_{n=1}^0, \quad \Delta P_{n=1}^{(1)}|_{\overline{\rm MS}} = -\frac{1}{8}\Delta\hat{\gamma}_{n=1}^{(1)}|_{\overline{\rm MS}}, \tag{C.11}$$

and using the information on the first moments of the anomalous dimensions which are listed in Appendices B.1 and B.2, we find that $M$ turns out to be a triangular matrix in the following form:

$$M = \begin{pmatrix} a & b & 0 \\ 0 & c & 0 \\ 0 & 0 & d \end{pmatrix}, \tag{C.12}$$

with

$$a = \frac{1}{\beta_0}\left[\frac{\alpha_s(0)}{\pi} - \frac{\alpha_s(t)}{\pi}\right]\left(-\frac{1}{8}\gamma^{(1),n=1}_{\psi\psi,\overline{\rm MS}}\right), \quad \text{(C.13)}$$

$$b = \frac{3}{2}C_F t + \frac{1}{\beta_0}\left[\frac{\alpha_s(0)}{\pi} - \frac{\alpha_s(t)}{\pi}\right] \times \left(-\frac{1}{8}\gamma^{(1),n=1}_{G\psi,\overline{\rm MS}} - \frac{3\beta_1}{4\beta_0}C_F\right), \quad \text{(C.14)}$$

$$c = \frac{1}{2}\beta_0 t, \quad \text{(C.15)}$$

$$d = \frac{1}{\beta_0}\left[\frac{\alpha_s(0)}{\pi} - \frac{\alpha_s(t)}{\pi}\right]\left(-\frac{1}{8}\gamma^{(1),n=1}_{\rm NS,\overline{MS}}\right). \quad \text{(C.16)}$$

The matrix $\exp(M)$ is, therefore, written in the form

$$\exp(M) = \begin{pmatrix} {\rm e}^a & B & 0 \\ 0 & {\rm e}^c & 0 \\ 0 & 0 & {\rm e}^d \end{pmatrix}, \quad \text{(C.17)}$$

and thus we obtain from (C.7) and (C.9),

$$\Delta q^\gamma_{\rm S}(n=1,Q^2,P^2)|_{\overline{\rm MS}} = -\frac{3\alpha}{\pi}N_f\langle e^2\rangle \times\exp\left\{-\frac{1}{8\beta_0}\left[\frac{\alpha_s(0)}{\pi} - \frac{\alpha_s(t)}{\pi}\right]\Delta\gamma^{(1),n=1}_{\psi\psi,\overline{\rm MS}}\right\} \quad \text{(C.18)}$$

$$\approx -\frac{3\alpha}{\pi}N_f\langle e^2\rangle\left\{1 - \frac{2}{\beta_0}\left[\frac{\alpha_s(P^2)}{\pi} - \frac{\alpha_s(Q^2)}{\pi}\right]N_f\right\},$$

$$\Delta q^\gamma_{\rm NS}(n=1,Q^2,P^2)|_{\overline{\rm MS}} = -\frac{3\alpha}{\pi}N_f(\langle e^4\rangle - \langle e\rangle^2) \times\exp\left\{-\frac{1}{8\beta_0}\left[\frac{\alpha_s(0)}{\pi} - \frac{\alpha_s(t)}{\pi}\right]\Delta\gamma^{(1),n=1}_{\rm NS,\overline{MS}}\right\}$$

$$= -\frac{3\alpha}{\pi}N_f(\langle e^4\rangle - \langle e\rangle^2), \quad \text{(C.19)}$$

where in the last line we use the fact $\Delta\gamma^{(1),n=1}_{\rm NS,\overline{MS}} = 0$.

Incidentally, under the following approximation:

$$b \approx \frac{3}{2}C_F t, \quad a + c \approx c, \quad \text{(C.20)}$$

$B$ is evaluated as

$$B \approx b\left\{1 + \frac{1}{2}c + \frac{1}{3!}c^2 + \frac{1}{4!}c^3 + \cdots\right\} = \frac{b}{c}[{\rm e}^c - 1] \approx \frac{3C_F}{\beta_0}\left[\frac{\alpha_s(P^2)}{\alpha_s(Q^2)} - 1\right]. \quad \text{(C.21)}$$

This leads to the expression for the first moment of gluon distribution $\Delta G^\gamma(n=1,Q^2,P^2)|_{\overline{\rm MS}}$ given in (4.6).

## References


1. W.A. Bardeen, A.J. Buras, Phys. Rev. D **20**, 166 (1979)
2. D.W. Duke, J.F. Owens, Phys. Rev D **22**, 2280 (1980)
3. T. Uematsu, T.F. Walsh, Phys. Lett. B **101**, 263 (1981)
4. T. Uematsu, T.F. Walsh, Nucl. Phys. B **199**, 93 (1982)
5. G. Rossi, Phys. Rev. D **29**, 852 (1984)
6. M. Drees, R.M. Godbole, Phys. Rev. D **50**, 3124 (1994)
7. M. Glück, E. Reya, M. Stratmann, Phys. Rev. D **51**, 3220 (1995); Phys. Rev. D **54**, 5515 (1996); M. Glück, E. Reya, I. Schienbein, Phys. Rev. D **60**, 54019 (1999)
8. B.L. Ioffe, A. Oganesian, Z. Phys. C **69**, 119 (1995)
9. G.A. Schuler, T. Sjostrand, Phys. Lett. B **376**, 193 (1996)
10. P. Mathews, V. Ravindran, Int. J. Mod. Phys A **11**, 2783 (1996)
11. D.P. Barber, in Proceedings of the Zeuthen Workshop on the Prospects of Spin Physics at HERA, DESY 95-200, p. 76, edited by J. Blümlein, W.D. Nowak
12. M. Stratmann, W. Vogelsang, Z. Phys. C **74**, 641 (1997)
13. R.W. Brown, I.J. Muzinich, Phys. Rev. D **4**, 1496 (1971)
14. M.A. Ahmed, G.G. Ross, Phys. Lett. B **59**, 369 (1975)
15. K. Sasaki, Phys. Rev. D **22**, 2143 (1980)
16. A.V. Manohar, Phys. Lett. B **219**, 357 (1989)
17. S.D. Bass, Int. J. Mod. Phys. A **7**, 6039 (1992)
18. M. Stratmann, W. Vogelsang, Phys. Lett. B **386**, 370 (1996)
19. A.V. Efremov, O.V. Teryaev, Phys. Lett. B **240**, 200 (1990)
20. S. Narison, G.M. Shore, G. Veneziano, Nucl. Phys. B **391**, 69 (1993); G.M. Shore, G. Veneziano, Mod. Phys. Lett. A **8**, 373 (1993); Nucl. Phys. B **381**, 23 (1992)
21. A. Freund, L.M. Sehgal, Phys. Lett. B **341**, 90 (1994)
22. S.D. Bass, S.J. Brodsky, I. Schmidt, Phys. Lett. B **437**, 424 (1998)
23. K. Sasaki, T. Uematsu, Phys. Rev. D **59**, 114011 (1999); Nucl. Phys. B (Proc. Suppl.) **79**, 614 (1999)
24. G. Altarelli, Phys. Rep. **81**, 1 (1982)
25. SMC, B. Adeva et al., Phys. Rev. D **58**, 112001 (1998); SLAC/E143 Collaboration, K. Abe et al., Phys. Rev. D **58**, 112003 (1998); HERMES Collaboration, A. Airapetian et al., Phys. Lett. B **442**, 484 (1998); SLAC/E155 Collaboration, P.L. Anthony et al., Phys. Lett. B **463**, 339 (1999)
26. M. Glück, E. Reya, M. Stratmann, W. Vogelsang, Phys. Rev. D **53**, 475 (1996); T. Gehrmann, W.J. Stirling, Phys. Rev. D **53**, 6100 (1996); D. de Florian, O.A. Sampayo, R. Sassot, Phys. Rev. D **57**, 5803 (1998)
27. G. Altarelli, R.D. Ball, S. Forte, G. Ridolfi, Nucl. Phys B **496**, 337 (1997); Acta Phys. Pol. B **29**, 1145 (1998)
28. E. Leader, A.V. Sidrov, D.B. Stamenov, Phys. Rev. D **58**, 114028 (1998); Phys. Lett. B **445**, 232 (1998); B **462**, 189 (1999)
29. SMC, B. Adeva et al., Phys. Rev. D **58**, 112002 (1998); HERMES Collaboration, K. Ackerstaff et al., Phys. Lett. B **464**, 123 (1999)
30. J. Kodaira, Nucl. Phys. B **165**, 129 (1980)
31. G. Altarelli, G.G. Ross, Phys. Lett. B **212**, 391 (1988)
32. R.D. Carlitz, J.C. Collins, A.H. Mueller, Phys. Lett. B **214**, 229 (1988)
33. V. Efremov, O.V. Teryaev, JINR Report NO. E2-88-287, Dubna, 1988
34. G.T. Bodwin, J. Qiu, Phys. Rev. D **41**, 2755 (1990)
35. G. Altarelli, B. Lampe, Z. Phys. C **47**, 315 (1990)
36. R.D. Ball, S. Forte, G. Ridolfi, Phys. Lett. B **378**, 255 (1996)
37. H.-Y. Cheng, Int. J. Mod. Phys. A **11**, 5109 (1996); Phys. Lett. B **427**, 371 (1998)
38. D. Müller, O.V. Teryaev, Phys. Rev. D **56**, 2607 (1997)
39. M. Glück, E. Reya, A. Vogt, Phys. Rev. D **45**, 3986 (1992)
40. K. Sasaki, T. Uematsu, Phys. Lett. B **473**, 309 (2000); Nucl. Phys. B (Proc. Suppl.) **89**, 162 (2000)

41. W. Furmanski, R. Petronzio, Z. Phys. C **11**, 293 (1982)
42. M. Glück, E. Reya, Phys. Rev. D **28**, 2749 (1983)
43. M. Fontannaz, E. Pilon, Phys. Rev. D **45**, 382 (1992)
44. P. Aurenche, J.-P. Guillet, M. Fontannaz, Z. Phys. C **64**, 621 (1994)
45. J. Kodaira, S. Matsuda, T. Muta, K. Sasaki, T. Uematsu, Phys. Rev. D **20**, 627 (1979)
46. R. Mertig, W.L. van Neerven, Z. Phys. C **70**, 637 (1996)
47. W. Vogelsang, Phys. Rev. D **54**, 2023 (1996); Nucl. Phys. B **475**, 47 (1996)
48. EMC, J. Ashman et al., Nucl. Phys. B **238**, 1 (1990); Phys. Lett. B **206**, 364 (1988)
49. J. Kodaira, S. Matsuda, K. Sasaki, T. Uematsu, Nucl. Phys. B **159**, 99 (1979)
50. W. Vogelsang, Z. Phys. C **50**, 275 (1991)
51. M. Stratmann, A. Weber, W. Vogelsang, Phys. Rev. D **53**, 138 (1996)
52. E.B. Zijlstra, W.L. van Neerven, Nucl. Phys. B **417**, 61 (1994)
53. K. Sasaki, Prog. Theor. Phys. Suppl. **77**, 197 (1983)
54. W.A. Bardeen, Proceedings 10th International Symposium on Lepton and Photon Interaction at High Energies (Bonn, 1981), edited by W. Pfeil (Bonn University, 1981) p. 432
55. I. Antoniadis, G. Grunberg, Nucl. Phys. B **213**, 445 (1983)
56. D.W. Duke, Proceedings XIV International Symposium on Multiparticle Dynamics (Lake Tahoe, 1983) edited by P. Yager, J.F. Gunion (World Scientific, 1984) p. 124